QED calculation of the interelectron interaction in two- and three-electron ions

O. Yu. Andreev,[1] L. N. Labzowsky,[1] G. Plunien,[2] and G. Soff[2]
[1]*Institute of Physics, St. Petersburg State University 198904, Petershof, St. Petersburg, Russia*
[2]*Institut für Theoretische Physik, Technische Universität Dresden, Mommsenstraße 13, D-01062, Dresden, Germany*
(Received 26 March 2001; revised manuscript received 18 June 2001; published 19 September 2001)

Accurate QED evaluations of the one- and two-photon interelectron interaction for the configurations $1s_{1/2}2s_{1/2}\ ^1S_0$ and $1s_{1/2}2s_{1/2}\ ^3S_1$ in He-like ions and for the configurations $(1s)^2 2s_{1/2}$ and $(1s)^2 2p_{1/2}$ in Li-like ions with nuclear charge numbers $30 \leqslant Z \leqslant 92$ are performed. The three-photon interaction is also partly taken into account. The QED theory of these corrections is provided by the adiabatic *S* matrix and by the line-profile approach. The Coulomb gauge is employed. The results are compared with available experimental data and with different calculations.

DOI: 10.1103/PhysRevA.64.042513 PACS number(s): 31.30.Jv, 31.10.+z

I. INTRODUCTION

The energy levels of two-electron ions are currently under intensive experimental investigations [1–8], as are those of three-electron ions [9–11]. The deduced experimental data [9] for the splitting between the energy levels $(1s_{1/2})^2 2s_{1/2}$ and $(1s_{1/2})^2 2p_{1/2}$ in Li-like U are very accurate and therefore imply an excellent opportunity for tests of QED in the strong electric field of the nucleus. A considerable number of theoretical investigations was devoted to the evaluation of different QED corrections to the energy levels of He-like and Li-like ions. A two-electron character displays the Lamb shift screening corrections and the interelectron interaction corrections. The Lamb shift screening corrections, i.e., electron self-energy screening corrections and vacuum polarization screening corrections, were calculated in [12–14] for He-like ions and in [15–20] for Li-like ions.

The dominant two-electron contribution results from the first-order interelectron interaction. The QED evaluation of the first-order interelectron interaction correction is trivial; see, for example, [21]. The second-order correction is much more intricate. Many theoretical results for two- and three-electron ions were obtained within the framework of relativistic many-body perturbation theory (RMBPT) [22–24] and its generalizations, namely the relativistic all-order many-body theory (AO) [25]. Compared to the full QED calculation, the following contributions are omitted in RMBPT and AO: (i) negative-energy intermediate states, (ii) crossed photon interaction, and (iii) exact treatment of retardation. On the other hand, AO partly takes into account retardation and higher-order interactions, which may be important even for very high *Z* ions.

Full QED calculations of the second-order interelectron interaction were accomplished in recent years only for the ground state of He-like ions [26,27]. Recently, the full QED approach was applied also to the $(1s_{1/2})^2 2p_{1/2}$-$(1s_{1/2})^2 2s_{1/2}$ splitting in Li-like U [28,29] and to $n=2$ triplet states in He-like ions [30].

For the evaluation of the interelectron interaction corrections within the QED theory, we employ the adiabatic *S* matrix approach [31,32] in the Furry picture and the Feynman graph techniques for the bound electrons. Details of the application of this approach to the bound-state QED are provided in [33,34,21].

It is essential to distinguish the contributions of the ''irreducible'' and ''reducible'' graphs. In the irreducible graphs, the initial or ''reference'' state is omitted in the summations over intermediate atomic states. The contribution of the ''reference'' states is described by the reducible graphs. The reducible graphs are singular and for their regularization a special procedure is needed. In the framework of the adiabatic *S* matrix approach, this procedure was described in [35,21]. For few-electron atoms, the evaluation of reference-state corrections (RSC) is simpler when the energies of both electrons coincide (ground state) and becomes much more complicated for the case of nonequal electron energies (excited states). In the latter case, the direct adiabatic *S* matrix approach is hardly applicable. Therefore, for the evaluation of the RSC for nonequal energies we will use in this paper the ''line profile approach'' developed in [36].

Reference-state corrections for two-electron atoms were first introduced in [37]. An explicit expression for the Coulomb-Breit ''box'' correction for equal energies (e.g., for the ground state of the two-electron atom) was obtained in [35], and for nonequal energies in [38–40]. In the latter case, the line profile approach has been employed.

The corresponding expressions for the RSC in the Feynman gauge and within the Green-function approach were obtained in [41] for equal energies and in [42] for nonequal energies. Numerical calculations of the RSC for the ground state of two-electron ions in the Feynman gauge were presented in [26,27]. The numerical calculations of the Coulomb-Breit RSC for the $1s_{1/2}2s_{1/2}\ ^1S_0$, $1s_{1/2}2p_{1/2}\ ^3P_0$, and $1s_{1/2}2s_{1/2}\ ^3S_1$ two-electron configurations and partly for the $(1s)^2 2s_{1/2}$ and $(1s)^2 2p_{1/2}$ three-electron configurations were performed in [39,40]. The numerical results for the RSC for three-electron configurations are also given in [28].

For the sake of accuracy, we reproduced the results for the ground $(1s_{1/2})^2$ state and made a detailed comparison with the corresponding results in [27], where the Coulomb gauge was also used. The Coulomb-Coulomb interaction was reproduced with an accuracy of 0.01% for all *Z* values. The Coulomb-Breit part has been reproduced with an accuracy of 0.05% and the Breit-Breit part is reproduced with an accuracy of 0.1%. The small deviations are due to the different

numerical methods: in [27] the method of discretization of the radial Dirac equations was employed, while we used the B-spline approach in this paper.

The paper is organized as follows. In Sec. II, a general description of the adiabatic *S* matrix approach is given and its historical background is briefly indicated. In Secs. III and IV, the formulas for the irreducible contributions to the interelectron interaction in two- and three-electron ions are provided. In Sec. V, the line profile QED approach is formulated and its application to the evaluation of the reducible contributions to the interelectron interaction is described. In Sec. VI, the formulas for the reducible contributions in two- and three-electron ions are derived. Section VII is devoted to a discussion of the results and to a comparison with experimental data and with different theoretical calculations. In Appendix A, the application of the *S*-matrix theory to irreducible Feynman graphs is rigorously formulated. Some details of the numerical procedure and the accuracy estimates are presented in Appendix B.

II. ADIABATIC *S*-MATRIX APPROACH

For the calculations of the corrections to the energy levels, we use the adiabatic *S*-matrix approach first developed by Gell-Mann and Low [31] and generalized to a form suitable for QED calculations by Sucher [32]. This approach is based on the Furry picture [43], which describes the many-electron atom as a set of electrons, moving in the field of the nucleus and interacting with one another through the interaction with the electromagnetic field. The Hamiltonian of an atom in the second quantization representation is

$$\hat{H}=\hat{H}_0+\hat{H}_{\rm int}, \tag{1}$$

$$\hat{H}_0=\int \hat{\Psi}^+(x)\hat{h}_D(\mathbf{r})\hat{\Psi}(x)d\mathbf{r}, \tag{2}$$

$$\hat{H}_{\rm int}=-\int \hat{j}_\mu(x)\hat{A}_\mu(x)d\mathbf{r}, \tag{3}$$

where $\hat{\Psi},\hat{\Psi}^+$ are the electron-positron field operators and $\hat{h}_D$ is the one-electron Dirac operator. $\hat{H}_{\rm int}$ defines the interaction of the electrons with the electromagnetic field, $\hat{j}_\mu$ is the operator of the electron-positron current, and $\hat{A}_\mu$ is the operator of the 4-vector potential of the electromagnetic field.

The Dirac operator $\hat{h}_D$ is given by

$$\hat{h}_D(\mathbf{r})=\boldsymbol{\alpha}\mathbf{p}+\beta m-eU_{\rm c}(\mathbf{r}), \tag{4}$$

where $\boldsymbol{\alpha},\beta$ are Dirac matrices, $\mathbf{p}\equiv -i\boldsymbol{\nabla}$, $U_{\rm c}(\mathbf{r})$ is the nuclear Coulomb potential, and m,e are the mass and the charge of the electron, respectively. We use the units $\hbar=c=1$.

Equations (3) and (4) define the Coulomb zero-order approximation. This approximation is most adequate for highly charged, few-electron ions. The basis set of the one-electron wave functions is defined by the wave equation

$$\hat{h}_{\rm D}\psi_n=\varepsilon_n\psi_n, \tag{5}$$

where ε_n are the one-electron energies. The zero-order wave function of the atom (ion) in the nondegenerate case is the Slater determinant built from the one-electron functions ψ_n $(n=1,\ldots,N)$, where N is the number of electrons. The zero-order energy of the atom is the sum of the one-electron energies

$$E^{(0)}=\sum_{n=1}^{N}\varepsilon_n. \tag{6}$$

The adiabatic *S*-matrix formalism is based on the use of the adiabatic evolution operator $\hat{S}_\lambda(t,t')$. This operator is expressed as

$$\hat{S}_\lambda(t,t')=1+\sum_{n=1}^{\infty}\hat{S}_\lambda^{(n)}(t,t'), \tag{7}$$

$$\hat{S}_\lambda^{(n)}(t,t')=(-i)^n e^n\int_{t'}^{t}\hat{H}_{\rm int}^{(\lambda)}(t_1)dt_1 \times\int_{t'}^{t_1}\hat{H}_{\rm int}^{(\lambda)}(t_2)dt_2\cdots\int_{t'}^{t_{n-1}}\hat{H}_{\rm int}^{(\lambda)}(t_n)dt_n, \tag{8}$$

$$\hat{H}_{\rm int}^{(\lambda)}(t)=e^{i\hat{H}_0 t}\hat{H}_{\rm int}e^{-i\hat{H}_0 t}e^{-\lambda|t|}. \tag{9}$$

Here $\lambda>0$ is the adiabatic parameter and $\hat{H}_{\rm int}^{(\lambda)}(t)$ denotes the adiabatic interaction Hamiltonian in the interaction representation. Formulas (7)–(9) present the adiabatic perturbation theory in powers of the interaction constant $e=\sqrt{\alpha}$ (α is the fine-structure constant).

Gell-Mann and Low [31] derived a formula which yields the energy shift due to the interaction (3) in terms of the operator $\hat{S}_\lambda(0,-\infty)$. Later Sucher [32] derived a symmetrized version of the energy shift formula, containing the matrix elements of the operator $\hat{S}(\infty,-\infty)$ and which is more suitable for the renormalization procedure. The energy shift is determined by

$$\Delta E_a=\lim_{\lambda\to 0}\frac{i}{2}\lambda e\frac{\frac{\partial}{\partial e}\langle\Phi_a|\hat{S}_\lambda(\infty,-\infty)|\Phi_a\rangle}{\langle\Phi_a|\hat{S}_\lambda(\infty,-\infty)|\Phi_a\rangle}, \tag{10}$$

where $|\Phi_a\rangle$ is the state vector for the noninteracting electron-positron and electromagnetic fields.

Formula (10) enables one to extend the well-known technique of calculating the *S*-matrix elements in QED to the energy shift calculations. Practically, this means that the Feynman graph technique in the Furry representation can be used for the calculation of the matrix elements of the adiabatic *S*-matrix in Eq. (10). All the time integrations should be done explicitly, and unlike the standard QED for the free electrons each vertex should contain the adiabatic exponent. This program was first realized in [33] where the QED theory of the interelectron interaction in many-electron atoms was considered.

For actual calculation it is convenient to expand Eq. (10) in powers of *e*. The corresponding expansion up to fourth order was given in [33]:

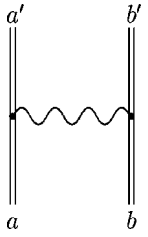

FIG. 1. A Feynman graph, describing the first-order interelectron interaction. The double solid line corresponds to bound electrons in the field of the nucleus, the wavy line corresponds to the sum of the Coulomb and Breit (transverse) photons. If $a'=a$ and $b'=b$, the graph is called ''direct''; when $a'=b$, $b'=a$ we call it an ''exchange'' graph. The latter name should be understood in connection with permutation symmetry.

$$\Delta E_a = \lim_{\lambda\to 0} \frac{1}{2} i\lambda \{ \langle \Phi_a | \hat{S}_\lambda^{(1)} | \Phi_a \rangle + [2\langle \Phi_a | \hat{S}_\lambda^{(2)} | \Phi_a \rangle - \langle \Phi_a | \hat{S}_\lambda^{(1)} | \Phi_a \rangle^2] + [3\langle \Phi_a | \hat{S}_\lambda^{(3)} | \Phi_a \rangle - 3\langle \Phi_a | \hat{S}_\lambda^{(2)} | \Phi_a \rangle \times \langle \Phi_a | \hat{S}_\lambda^{(1)} | \Phi_a \rangle + \langle \Phi_a | \hat{S}_\lambda^{(1)} | \Phi_a \rangle^3] + [4\langle \Phi_a | \hat{S}_\lambda^{(4)} | \Phi_a \rangle - 4\langle \Phi_a | \hat{S}_\lambda^{(3)} | \Phi_a \rangle \langle \Phi_a | \hat{S}_\lambda^{(1)} | \Phi_a \rangle + 4\langle \Phi_a | \hat{S}_\lambda^{(2)} | \Phi_a \rangle \times \langle \Phi_a | \hat{S}_\lambda^{(1)} | \Phi_a \rangle^2 - 2\langle \Phi_a | \hat{S}_\lambda^{(2)} | \Phi_a \rangle^2 - \langle \Phi_a | \hat{S}_\lambda^{(1)} | \Phi_a \rangle^4] \}. \tag{11}$$

For irreducible matrix elements the procedure of the evaluation of the limit $\lambda\to 0$ can be avoided and the adiabatic formula can be replaced by a simpler one [44,21],

$$\Delta E_a^{(n,\mathrm{irr})} = \langle \Phi_a | U^{(n)} | \Phi_a \rangle, \tag{12}$$

where the ''effective potential energy'' $U^{(n)}$ is defined as

$$\langle \Phi_b | \hat{S}^{(n)} | \Phi_a \rangle_{\mathrm{irr}} = -2\pi i\, \delta(E_a^{(0)} - E_b^{(0)}) \langle \Phi_b | U^{(n)} | \Phi_a \rangle. \tag{13}$$

A simple proof of Eqs. (12) and (13) is given in Appendix A.

In principle, Eqs. (10) and (11) are valid for nondegenerate states only. For the generalization to the degenerate case, we refer to [21]. However, the formulas (10)–(13) remain unchanged in the most important case where the degenerate states differ by symmetry.

Details of the Feynman graph techniques for bound electrons can be found in [21,34]. Different QED approaches to the calculations with bound electrons in atoms, based on the Green-function method, were formulated in [45] and [41,46] (two-times Green-function method [47]).

III. IRREDUCIBLE CONTRIBUTIONS TO THE INTERELECTRON INTERACTION IN TWO-ELECTRON IONS

The first-order interelectron interaction for two-electron configurations is described by the Feynman graph of Fig. 1. This graph is irreducible.

In Fig. 2, the second-order interelectron interaction Feynman graphs are depicted. The ''box'' graph [Fig. 2(a)] is reducible. They have singularities when $\varepsilon_{n_1}+\varepsilon_{n_2}=\varepsilon_a+\varepsilon_b$. In this section we will consider only the ''irreducible'' part of these reducible graphs, that is, the contribution from $\varepsilon_{n_1}+\varepsilon_{n_2}\neq\varepsilon_a+\varepsilon_b$. The ''crossed'' graph in Fig. 2 is irreducible. However, usually one extracts the terms with $\varepsilon_{n_1}+\varepsilon_{n_2}=\varepsilon_a+\varepsilon_b$ (which are not singular) from this graph and considers these terms together with the ''reducible'' parts of the ''box'' graph. One of the reasons is that the Coulomb-Breit reducible corrections for the ''box'' and ''crossed'' graphs cancel each other in the case of equal energies (ground state). We will follow this tradition in our paper and thus we divide the contributions of the ''crossed'' graphs into ''irreducible'' and ''reducible'' parts.

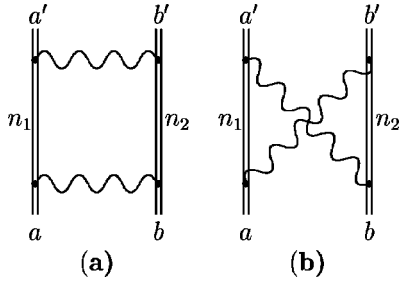

FIG. 2. Notations are the same as in Fig. 1. By n_1,n_2 the summation over the intermediate states is denoted. Graph (a) is called a ''box'' and graph (b) is called a ''cross'' graph.

According to the correspondence rules for Feynman graphs in bound-state QED [21,34], the electron propagator can be expressed as [48]

$$S(x_1,x_2) = \frac{1}{2\pi i}\int_{-\infty}^{\infty} d\omega\, e^{i\omega(t_1-t_2)} \sum_n \frac{\psi_n(\mathbf{r}_1)\overline{\psi}_n(\mathbf{r}_2)}{\varepsilon_n(1-i0)+\omega}, \tag{14}$$

where $x\equiv(\mathbf{r},it)$, $\overline{\psi}_n$ is the Dirac conjugate function, and the summation extends over the whole Dirac spectrum for the bound electron.

The photon propagators for the Coulomb and transverse photons are given by [21,34]

$$D^{c,t}_{\mu_1\mu_2}(x_1,x_2) = \frac{1}{2\pi i}\int_{-\infty}^{\infty} d\Omega\, I^{c,t}_{\mu_1\mu_2}(\Omega,r_{12}) e^{i\Omega(t_1-t_2)} \tag{15}$$

with

$$I^{c}_{\mu_1\mu_2}(\Omega,r_{12}) = \frac{\delta_{\mu_1 4}\delta_{\mu_2 4}}{r_{12}}, \quad r_{12}=|r_1-r_2| \tag{16}$$

and

$$I^{t}_{\mu_1\mu_2}(\Omega,r_{12}) = \left(\frac{\delta_{\mu_1\mu_2}}{r_{12}} e^{i|\Omega|r_{12}} + \boldsymbol{\nabla}_{1\mu_1}\cdot\boldsymbol{\nabla}_{2\mu_2}\frac{1}{r_{12}}\frac{1-e^{i|\Omega|r_{12}}}{|\Omega^2|} \right) \times (1-\delta_{\mu_1 4})(1-\delta_{\mu_2 4}). \tag{17}$$

Two-electron configurations are described by the wave function

$$\Psi_{JMj_1j_2l_1l_2}(\mathbf{r}_1,\mathbf{r}_2) = N\sum_{m_1m_2} C^{j_1j_2}_{JM}(m_1m_2)[\psi_{j_1l_1m_1}(\mathbf{r}_1)\psi_{j_2l_2m_2}(\mathbf{r}_2) - \psi_{j_1l_1m_1}(\mathbf{r}_2)\psi_{j_2l_2m_2}(\mathbf{r}_1)], \quad (18)$$

where $N=1/2$ for equivalent electrons and $N=1/\sqrt{2}$ for nonequivalent electrons; $C^{j_1j_2}_{JM}(m_1m_2)$ is a Clebsh-Gordan symbol. It follows from Eq. (18) that for configuration $1s2s\ ^3S_1$ the energy corrections are given directly by the following formula with $a,b=1s_+,2s_+$, where $\pm$ denote the two different projections of the total electron angular momentum:

$$\Delta E(1s2s\ ^3S_1)=F_{1s_+2s_+;1s_+2s_+}, \quad (19)$$

where

$$F_{ab;cd}=F_{abcd}-F_{bacd}, \quad (20)$$

$F_{ab\ldots}$ is a function of one-electron states, which are described by wave functions $\psi_a,\psi_b,\ldots$. The form of the function F depends on the type of the considered Feynman graph (see below). For the configuration $1s2s\ ^1S_0$ the energy correction is given by

$$\Delta E(1s2s\ ^1S_0)=F_{1s_-2s_+;1s_-2s_+}-F_{1s_+2s_-;1s_-2s_+}. \quad (21)$$

The graph in Fig. 1 is irreducible and one can apply the formulas (12) and (13) for the evaluation of the energy corrections. Then using the correspondence rules for the bound-state QED, inserting the expressions for the propagators into the S-matrix elements, and integrating over the time and frequency variables one obtains

$$F^{(1)}_{a'b'ab}=\sum_g I^g(\varepsilon_{a'}-\varepsilon_a)_{a'b'ab}. \quad (22)$$

Here we have introduced the following abbreviation [see definitions (16) and (17)]:

$$I^g_{a'b'ab}(\Omega)\equiv\sum_{\mu_1\mu_2}\int \overline{\psi}_{a'}(\mathbf{r}_1)\overline{\psi}_{b'}(\mathbf{r}_2)\gamma^{(1)}_{\mu_1}\gamma^{(2)}_{\mu_2}I^g_{\mu_1\mu_2}(\Omega,r_{12}) \times\psi_a(\mathbf{r}_1)\psi_b(\mathbf{r}_2)d\mathbf{r}_1d\mathbf{r}_2, \quad (23)$$

where the Dirac matrices $\gamma^{(i)}_{\mu_i}$ are acting on the wave functions depending on the variables $\mathbf{r}_i$. Then $g=c,t$. For $g=c$, Eq. (22) determines the first-order Coulomb correction and for $g=t$ we obtain the first-order Breit correction.

The same sequence of operations that was used for the derivation of the first-order correction [the correspondence rules for the graphs Fig. 2, time and frequency integrations, use of Eqs. (12) and (13)] should be repeated for the evaluation of the irreducible contributions of the second-order corrections.

For the ''box'' and ''cross'' corrections, the results are

$$F^{(2)(\mathrm{box,irr})}_{a'b'ab}=\sum_{gg'}{\sum_{n_1n_2}}'\left\{\frac{i}{2\pi}\int_{-\infty}^{\infty}\frac{I^g(\Omega)_{a'b'n_1n_2}I^{g'}(\Omega-\varepsilon_{a'}+\varepsilon_a)_{n_1n_2ab}}{(\varepsilon_a+\varepsilon_b-\varepsilon_{n_1}-\varepsilon_{n_2})(\Omega-\varepsilon_{n_2}+\varepsilon_{b'}+i0\varepsilon_{n_2})}d\Omega + \frac{i}{2\pi}\int_{-\infty}^{\infty}\frac{I^g(\Omega)_{b'a'n_1n_2}I^{g'}(\Omega-\varepsilon_a+\varepsilon_{a'})_{n_1n_2ba}}{(\varepsilon_a+\varepsilon_b-\varepsilon_{n_1}-\varepsilon_{n_2})(\Omega-\varepsilon_{n_2}+\varepsilon_{a'}+i0\varepsilon_{n_2})}d\Omega\right\}, \quad (24)$$

$$F^{(2)(\mathrm{cross,irr})}_{a'b'ab}=\sum_{gg'}{\sum_{n_1n_2}}'\left\{\frac{i}{2\pi}\int_{-\infty}^{\infty}\frac{I^g(\Omega)_{b'n_2n_1a}I^{g'}(\Omega-\varepsilon_{a'}+\varepsilon_a)_{n_1a'bn_2}}{(\varepsilon_{n_2}-\varepsilon_{n_1}-\varepsilon_a+\varepsilon_{b'})(\Omega-\varepsilon_{n_2}+\varepsilon_a+i0\varepsilon_{n_2})}d\Omega + \frac{i}{2\pi}\int_{-\infty}^{\infty}\frac{I^g(\Omega)_{n_1b'an_2}I^{g'}(\Omega-\varepsilon_a+\varepsilon_{a'})_{a'n_2n_1b}}{(\varepsilon_{n_2}-\varepsilon_{n_1}+\varepsilon_a-\varepsilon_{b'})(\Omega-\varepsilon_{n_2}+\varepsilon_{b'}+i0\varepsilon_{n_2})}d\Omega\right\}, \quad (25)$$

where the prime at the sum symbols means that the summation runs over n_1,n_2 except for the case when $n_1=a,n_2=b$ or $n_1=b,n_2=a$ (reference states). It should be stressed that in order to avoid division by zero in Eq. (25) in the case $a=b'$ and $n_1=n_2$, one has either to take the limit $n_1\to n_2$ for both terms on the right-hand side of the equation (the singularities cancel) or to use the formulas given in Sec. VI. When $g=g'=c$, we have the Coulomb-Coulomb correction,

when $g=g'=t$ we have the Breit-Breit, and the case $g=c,g'=t$ or $g=t,g'=c$ corresponds to the Coulomb-Breit interaction.

In some cases (see Sec. VII) the accuracy of the experiments requires the inclusion of the third-order interelectron interaction corrections in the theoretical evaluations. Still the third-order contribution for high-Z ions is small and it is sufficient to take into account only the dominant part of this contribution, that is, the third-order Coulomb and unretarded Breit ''box'' corrections. The corresponding Feynman graph is displayed in Fig. 3. The formula for the irreducible part of the third-order ''box'' correction, derived in the same way as the corrections (22) and (24), can be expressed as

$$F^{(\mathrm{box,irr})}_{a'b'ab}=\sum_{gg'g''}\sum_{n_1n_2n_3n_4}{}' \frac{I^{g}_{a'b'n_3n_4}I^{g'}_{n_3n_4n_1n_2}I^{g''}_{n_1n_2ab}}{(\varepsilon_{n_3}+\varepsilon_{n_4}-\varepsilon_{a'}-\varepsilon_{b'})(\varepsilon_{n_1}+\varepsilon_{n_2}-\varepsilon_{a}-\varepsilon_{b})}, \tag{26}$$

where the prime indicates that the summation is not running over the reference states.

IV. IRREDUCIBLE CONTRIBUTIONS TO THE INTERELECTRON INTERACTION IN THREE-ELECTRON IONS

The first-order interelectron interaction in three-electron ions is described again by Fig. 1. The second-order interaction partly is described also by the same graphs, Fig. 2, as for the two-electron case. We will consider two three-electron configurations: the ground state $(1s_{1/2})^2 2s_{1/2}$ and the first excited state $(1s_{1/2})^2 2p_{1/2}$. In the former case, the indices a, b run over the set $1s_+,1s_-,2s_+$ and in the latter case they run over the set $1s_+,1s_-,2p_{1/2+}$, where $\pm$ denote the total angular momentum projections. Apart from the graphs in Fig. 2, for three-electron ions we have to consider the ''step'' graphs depicted in Figs. 4 and 5. For the ''step'' graph in the case of the configuration $(1s_{1/2})^2 2s_{1/2}$, the indices a,b,c run over the set $1s_+,1s_-,2s_+$, and in the case of the configuration $(1s_{1/2})^2 2p_{1/2}$ the indices a,b,c run over the set $1s_+,1s_-,2p_{1/2+}$.

The first-order contribution, as well as the second-order ''box,'' ''cross,'' and third-order ''box'' contributions, can be represented as

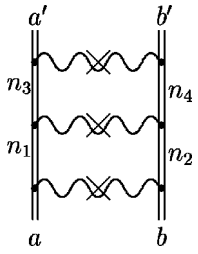

FIG. 3. The third-order ''box'' Feynman graph. The notations are the same as in Figs. 1 and 2. Here the wavy line with the cross denotes the sum of the Coulomb and unretarded Breit interaction.

$$\Delta E_{abc}=F_{ab;ab}+F_{bc;bc}+F_{ca;ca}, \tag{27}$$

where $F_{ab;cd}$ is given by Eqs. (23), (22), (24), (25), and (26).

The contributions of the ''step'' graphs in Fig. 4 can be obtained by the formula

$$\Delta E_{abc}=\sum_{\substack{i',j',k'=1,2,3\\ i,j,k=1,2,3}} \epsilon_{i'j'k'}\,\epsilon_{ijk}F_{i'j'k'ijk}, \tag{28}$$

where the states a,b,c are denoted as 1,2,3 and ϵ_{ijk} is the unit antisymmetric tensor. Equation (28) includes the contribution of the ''direct'' and all the possible ''exchange'' graphs in the three-electron case. The quantity $F^{(\mathrm{step,irr})}_{a'b'c'abc}$ is defined as

$$F^{(\mathrm{step,irr})}_{a'b'c'abc}=\sum_{gg'}\sum_{n}{}' \frac{I^{g}(\varepsilon_a-\varepsilon_{a'})_{na'ba}I^{g'}(\varepsilon_{c'}-\varepsilon_c)_{b'c'nc}}{\varepsilon_a+\varepsilon_b-\varepsilon_{a'}-\varepsilon_n}, \tag{29}$$

where the prime at the sum means that the summation runs over all n except the case when the set of one-electron states $\{a',n,c\}$ is equivalent to the set $\{a,b,c\}$ (the case of reference states). This leads to the condition $\varepsilon_a+\varepsilon_b-\varepsilon_{a'}-\varepsilon_n \neq 0$. Thus we omit the singular term in the n summation (see Fig. 4) that gives rise to the ''reducible'' contribution. As in Sec. III, here $g,g'=c,t$. The reducible contribution does not arise for $g=g'=c$.

It remains to consider the third-order Coulomb and unretarded Breit corrections for three-electron ions. The corre-

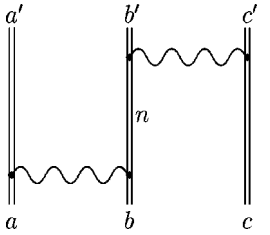

FIG. 4. The second-order ''step'' graph for three-electron atoms. The notations are the same as in Figs. 1 and 2.

sponding ''step-box'' graphs that yield the main contribution to the three-electron interaction are depicted in Fig. 5. The contribution of these graphs $\Delta E^{(\text{step-box})}_{abc}$ is described by the same formula (28) as $\Delta E^{(\text{step})}_{abc}$. It is easy to find out that the contributions of graphs Figs. 5(b) and 5(c) are equal. Therefore, we will consider the contributions of these graphs as the doubled contribution of a graph, Fig. 5(b). The quantity $F^{(\text{step-box,irr})}_{a'b'c'abc}$ is given by the formula

$$F^{(3)(\text{step-box,irr})}_{a'b'c'abc} = \sum_{gg'g''} {\sum_{n_1n_2n_3}}' \frac{I^{g}_{a'b'n_1n_3} I^{g'}_{n_3c'n_2c} I^{g''}_{n_1n_2ab}}{(\varepsilon_{n_1}+\varepsilon_{n_3}-\varepsilon_{a'}-\varepsilon_{b'})(\varepsilon_{n_1}+\varepsilon_{n_2}-\varepsilon_a-\varepsilon_b)}$$

$$+2\sum_{gg'g''} {\sum_{n_1n_2n_3}}' \frac{I^{g}_{b'c'n_3c} I^{g'}_{a'n_3n_1n_2} I^{g''}_{n_1n_2ab}}{(\varepsilon_{n_1}+\varepsilon_{n_2}-\varepsilon_a-\varepsilon_b)(\varepsilon_{n_3}+\varepsilon_{a'}-\varepsilon_a-\varepsilon_b)}$$

$$+\sum_{gg'g''} {\sum_{n_1n_2n_3}}' \frac{I^{g}_{a'c'n_1n_3} I^{g'}_{b'n_3n_2c} I^{g''}_{n_1n_2ab}}{(\varepsilon_{n_1}+\varepsilon_{n_2}-\varepsilon_a-\varepsilon_b)(\varepsilon_{n_1}+\varepsilon_{n_3}-\varepsilon_{a'}-\varepsilon_{c'})}, \tag{30}$$

where the prime at the sum symbols indicates that the first summation does not run over the states for which either the set $\{n_1,n_2,c\}$ or the set $\{n_1,n_3,c'\}$ are equivalent to the set $\{a,b,c\}$, the second summation does not run over the states for which the sets $\{n_1,n_2,c\}$ or $\{a',n_3,c\}$ are equivalent to the set $\{a,b,c\}$ and the third summation does not run over the states for which the sets $\{n_1,n_2,c\}$ or $\{n_1,n_3,b'\}$ are equivalent to the set $\{a,b,c\}$ (the cases of reference states).

V. LINE PROFILE APPROACH

The problem of the natural line profile in atomic physics was considered first in terms of quantum mechanics by Weisskopf and Wigner [49]. In terms of modern QED, it was first formulated for one-electron atoms by Low [50]. In [50], the appearance of the Lorentz profile in the resonance approximation within the framework of QED was described and the nonresonant corrections were estimated. Later the line profile QED theory was modified also for two-electron atoms [51] (see also [21,34]) and applied to the theory of overlapping resonances in two-electron highly charged ions [52,53]. Another application was provided to the theory of nonresonant corrections in highly charged ions [54,55].

It was found in [36] that the line profile approach (LPA) provides a convenient tool for calculating the energy corrections. It clearly indicates the limits up to which the concept of the energy of the excited states has a physical meaning, that is, the resonance approximation. The exact theoretical value for the energy of the excited state defined, for example, by the Green-function pole can be compared directly with the measurable quantities only in the resonance approximation when the following line profile is described by the following two parameters: energy E and width Γ. Beyond this

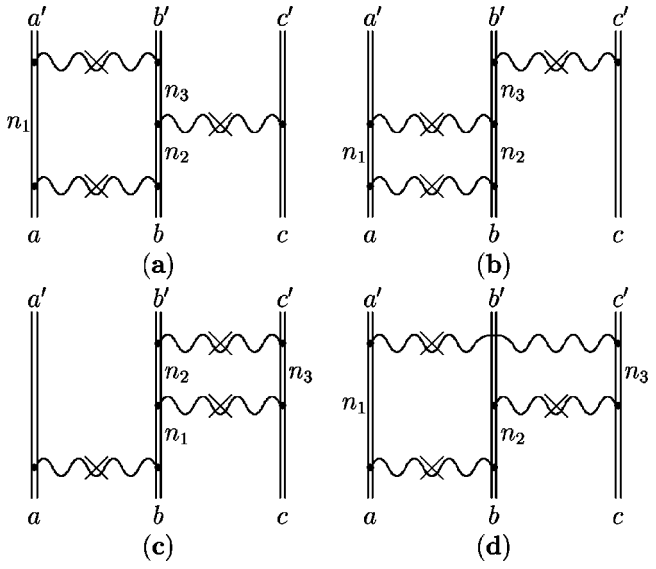

FIG. 5. The third-order ''step-box'' graphs. The notations are the same as in Figs. 1, 2, and 3. The wavy line with the cross denotes the sum of the Coulomb and unretarded Breit interactions.

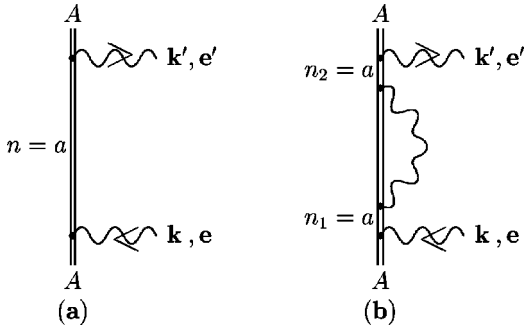

FIG. 6. The lowest-order amplitude of the photon scattering on the atomic electron in the resonance approximation (a) and insertion of the self-energy part into the photon scattering graph in the resonance approximation (b). The wavy lines with the arrows denote the absorption or the emission of the photon with momentum **k** and polarization **e**.

approximation, the evaluation of E and Γ should be replaced by the evaluation of the line profile for the particular process. Moreover, the line profile approach was found to be very useful for the evaluation of the reference-state (reducible) correction in the case of two-electron atoms. In the nonequal energy case, the use of the line profile theory appeared to be much simpler than the employment of the adiabatic formula (11).

Consider first the simplest process of photon scattering on the one-electron ion [Fig. 6(a)], which is assumed to be in its ground state A. Using the correspondence rules, we obtain the expression for the scattering amplitude,

$$U_A^{(2)}=e^2\sum_n \frac{[\gamma_\nu A_\nu(\mathbf{k}',\mathbf{e}')^*]_{An}[\gamma_\mu A_\mu(\mathbf{k},\mathbf{e})]_{nA}}{\varepsilon_n-\varepsilon_A-\omega}, \quad (31)$$

where $A_\mu(\mathbf{k},\mathbf{e})$ is the potential of the electromagnetic field. The frequencies of the absorbed and emitted photons are $\omega=|\mathbf{k}|$ and $\omega'=|\mathbf{k}'|=\omega$, respectively. We will consider the resonance case when the frequency ω is close to the value $\omega^{\rm res}=\varepsilon_a-\varepsilon_A+O(\alpha)$, where a is one of the excited states of an atom. In the framework of this resonance approximation, we have to retain only one term in the sum over n in Eq. (31): $n=a$. This is shown in Fig. 6a. Then

$$U_{Aa}^{(2)}=e^2\frac{[\gamma_\nu A_\nu(\mathbf{k}',\mathbf{e}')^*]_{Aa}[\gamma_\mu A_\mu(\mathbf{k},\mathbf{e})]_{aA}}{\varepsilon_a-\varepsilon_A-\omega}. \quad (32)$$

To obtain the Lorentz contour, one has to insert the electron self-energy part in the internal electron line in Fig. 6(a). For simplicity, we neglect the vacuum polarization part. In lowest order this leads to Fig. 6(b) and the expression for the scattering amplitude in the resonance approximation will be

$$U_{Aa}^{(4)}=U_{Aa}^{(2)}\frac{-v_1(\omega)}{\varepsilon_a-\varepsilon_A-\omega}, \quad (33)$$

where

$$v_1(\omega)=e^2[\hat{\Sigma}_R(\omega+\varepsilon_A)]_{aa}. \quad (34)$$

Here $\hat{\Sigma}_R(\omega)$ is the renormalized electron self-energy operator. The lower index at the function v indicates the order in α for the graphs which contribute to this function. Repeating these insertions in higher orders, we can obtain the geometric progression with the nth member,

$$q_n=U_{Aa}^{(2)}\left(\frac{-v_1(\omega)}{\varepsilon_a-\varepsilon_A-\omega}\right)^n. \quad (35)$$

Summing up this progression, we will get

$$U_{Aa}=e^2\frac{[\gamma_\nu A_\nu(\mathbf{k}',\mathbf{e}')^*]_{Aa}[\gamma_\mu A_\mu(\mathbf{k},\mathbf{e})]_{aA}}{\varepsilon_a-\varepsilon_A+v_1(\omega)-\omega}. \quad (36)$$

Taking the square modulus of the amplitude (36), integrating over the directions of the absorbed and emitted photons, and summing over the polarizations we obtain the Lorentz profile for the absorption probability,

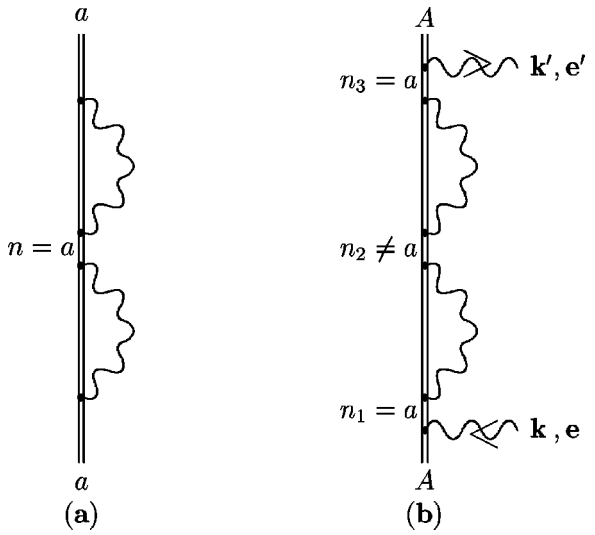

FIG. 7. Reducible Feynman graph SESE (loop after loop) (a) that gives rise to the correction in Eq. (44)(a) and the Feynman graph (b) representing the higher-order electron self-energy correction within the line profile approach (SESE, loop after loop, irreducible).

$$dW(\omega)=\frac{1}{2\pi}\frac{\Gamma_{aA}}{[\varepsilon_a-\varepsilon_A+\mathrm{Re}\{v_1(\omega)\}-\omega]^2+[\mathrm{Im}\{v_1(\omega)\}]^2}d\omega. \quad (37)$$

Here $dW(\omega)$ is the probability of the photon absorption in the frequency interval ω, $\omega+d\omega$ and Γ_{aA} is the partial width of the level a, connected with the transition $a\to A$.

Taking into account the graph Fig. 6(b), we improve the position of the resonance,

$$\omega^{\rm res}=\varepsilon_a-\varepsilon_A+\mathrm{Re}\{v_1(\varepsilon_a-\varepsilon_A)\}+O(\alpha^2). \quad (38)$$

We define the energy shift as the shift of the resonance. Then the real part of the matrix element $[\hat{\Sigma}_R(\varepsilon_a)]_{aa}$ gives the lowest-order contribution to the Lamb shift, and the imaginary part which is finite and not subject to renormalization gives the total radiative (single-quantum) width of the level a:

$$\Delta E_a^{\rm SE}=[\hat{\Sigma}_R(\varepsilon_a)]_{aa}=L_a^{\rm SE}-\frac{i}{2}\Gamma_a. \quad (39)$$

The other contribution to the lowest-order Lamb shift $L_a^{\rm VP}$ originates from the vacuum polarization graph. This graph gives no contribution to the width Γ_a [21].

The insertion of the Lamb shift L_A, corresponding to the ground state A into the Lorentz profile (37), is a more complicated problem, but can also be done within the approach developed in [51]. The line profile for the emission process $a\to A$ is described again by Eq. (37).

If we were to study the higher-order Lamb shift in one-electron atoms by the line profile approach, we would have to consider next the Feynman graph in Fig. 7(a) (for simplic-

ity, we will not consider the other second-order graphs). If $n_1=n_3=a$ and $n_2\neq a$, the graph of Fig. 7(a) can be considered as a complicated insertion represented by Fig. 7(b) in the graph of Fig. 6(a) in the resonance approximation. We get the following expression for the scattering amplitude:

$$U_{Aa}^{(6)}=U_{Aa}^{(2)}\frac{-v_2(\omega)}{\varepsilon_a-\varepsilon_A-\omega}, \tag{40}$$

where

$$v_2(\omega)=e^4\sum_{n\neq a}\frac{[\hat{\Sigma}_R(\omega+\varepsilon_A)]_{an}[\hat{\Sigma}_R(\omega+\varepsilon_A)]_{na}}{\varepsilon_A-\varepsilon_n+\omega}. \tag{41}$$

Note that the singular term $n=a$ is not included here by definition. This term was taken into account in the geometric progression described above and presents exactly the second member of this progression. Then repeating the evaluations leading to Eq. (37) with

$$q_n=U_{Aa}^{(2)}\left(\frac{-v_1(\omega)-v_2(\omega)}{\varepsilon_a-\varepsilon_A-\omega}\right)^n, \tag{42}$$

we obtain the new resonance condition,

$$\varepsilon_a-\varepsilon_A+\mathrm{Re}\{v_1(\omega)+v_2(\omega)\}+O(\alpha^3)-\omega=0. \tag{43}$$

Resolving Eq. (43), we find

$$\omega^{\mathrm{res}}=\varepsilon_a-\varepsilon_A+\mathrm{Re}\left\{v_1(\varepsilon_a-\varepsilon_A)+v_2(\varepsilon_a-\varepsilon_A)+v_1(\varepsilon_a-\varepsilon_A)\left[\frac{\partial v_1(\omega)}{\partial\omega}\right]_{\omega=\varepsilon_a-\varepsilon_A}\right\}+O(\alpha^3). \tag{44}$$

The term $v_2(\varepsilon_a-\varepsilon_A)$ is the contribution of the irreducible part of graph Fig. 7(a). The term with the derivative coincides with the reducible (or reference-state) correction that arises from the Feynman graph in Fig. 7(a) after the application of the adiabatic S-matrix formula (11) [56]. The other second-order electron self-energy (SESE) corrections are irreducible [56]. The calculation of all these corrections is not a subject of this paper.

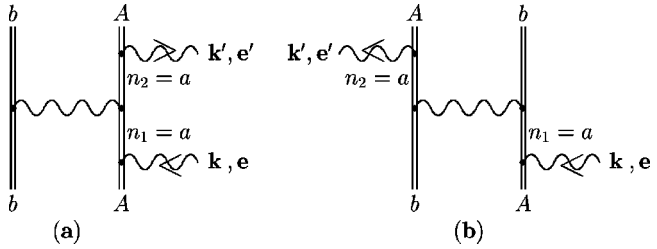

FIG. 8. First-order interelectron interaction correction to the scattering amplitude in the resonance approximation. Graphs (a) and (b) correspond to ''direct'' and ''exchange'' insertions.

Now we can address the two-electron graphs. At first we consider the first-order interaction represented by Fig. 1. Within the framework of the line profile approach, this graph should be inserted into the graph in Fig. 6(a). In the resonance approximation, this is depicted in Fig. 8. To follow the LPA rigorously, we have to take into account simultaneously the first-order self-energy, vacuum polarization, Coulomb, and Breit graphs. Then the function $v_1(\omega)$ contains the sum of corresponding contributions. In principle, in the next order we have to take into account the graphs describing self-energy and vacuum polarization screening. These corrections are, however, beyond the scope of the present work. So we consider only two-electron one- up to three-photon exchange ''box'' graphs. The contribution of the ''cross'' graphs will be discussed below in Sec. VI. Following the procedure described above for the one-photon exchange, we get

$$v_1=e^2\sum_{g=c,t}I^g(\varepsilon_a-\varepsilon_A)_{abab}. \tag{45}$$

Here v_1 does not depend on ω.

For two-photon exchange in two-electron ions, we have to consider a complicated insertion represented in Fig. 9. Then the LPA yields

$$v_2(\omega)=\frac{e^4 i}{2\pi}\sum_{gg'}\sum_{\varepsilon_{n_3}+\varepsilon_{n_4}\neq\varepsilon_a+\varepsilon_b}\int_{-\infty}^{\infty}\frac{I^g(\Omega)_{abn_3n_4}I^{g'}(-\Omega)_{n_3n_4ab}}{[\varepsilon_{n_4}(1-i0)+\Omega-\varepsilon_b][\varepsilon_{n_3}(1-i0)-\Omega-\varepsilon_A-\omega]}d\Omega$$
$$-\frac{e^4 i}{2\pi}\sum_{gg'}\sum_{\varepsilon_{n_3}+\varepsilon_{n_4}=\varepsilon_a+\varepsilon_b}\int_{-\infty}^{\infty}\frac{I^g(\Omega)_{abn_3n_4}I^{g'}(-\Omega)_{n_3n_4ab}}{[\varepsilon_{n_3}(1-i0)-\Omega-\varepsilon_a][\varepsilon_{n_3}(1-i0)-\Omega-\varepsilon_A-\omega]}d\Omega. \tag{46}$$

The second term in Eq. (46) represents the remainder after the subtraction of the reference-state singularity from Eq. (46). This subtraction was done when the geometric progression with the one-photon exchange graphs was generated. In the one-electron case, the reference-state term in $v_2(\omega)$ was absent [see Eq. (41)] and appeared only as a term with a derivative in Eq. (44). In the two-electron case (for photon exchange), the situation is different. In this case, there is a reference-state contribution directly in $v_2(\omega)$ [see Eq. (46)], and since v_1 does not depend on ω, a term with a derivative does not arise.

Considering the three-photon exchange and disregarding the retardation, we get for $v_3(\omega)$ the expression

$$v_3(\omega)=\sum_{gg'g''}{\sum_{n_1n_2n_3n_4}}'\frac{I^g_{abn_3n_4}I^{g'}_{n_3n_4n_1n_2}I^{g''}_{n_1n_2ab}}{(\varepsilon_{n_3}+\varepsilon_{n_4}-\varepsilon_A-\varepsilon_b-\omega)(\varepsilon_{n_1}+\varepsilon_{n_2}-\varepsilon_A-\varepsilon_b-\omega)}, \tag{47}$$

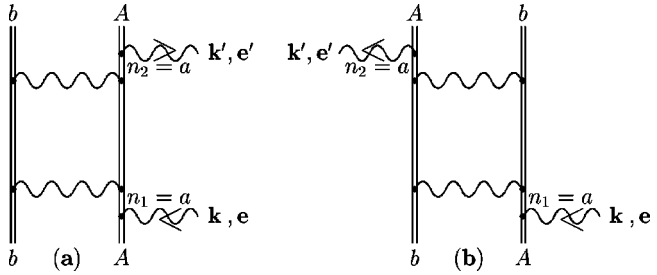

FIG. 9. Second-order interelectron interaction correction to the scattering amplitude in the resonance approximation. Graphs (a) and (b) correspond to ''direct'' and ''exchange'' insertions.

where the prime indicates that the summation is not running over the reference states.

All the geometric progressions considered above for two-electron graphs should be combined into one. Following this approach, we obtain the resonance condition

$$\varepsilon_a-\varepsilon_A+\mathrm{Re}\{v_1(\omega)+v_2(\omega)+v_3(\omega)\}+O(\alpha^4)-\omega=0. \tag{48}$$

We note that for two-electron graphs, describing photon exchange v_1 does not depend on ω. So solving Eq. (48) with v_1, v_2, and v_3 given by Eqs. (45), (46), and (47), we get

$$\omega^{\mathrm{res}}=\varepsilon_a-\varepsilon_A+\mathrm{Re}\Bigg\{v_1(\varepsilon_a-\varepsilon_A)+v_2(\varepsilon_a-\varepsilon_A)+v_3(\varepsilon_a-\varepsilon_A)+v_1(\varepsilon_a-\varepsilon_A)\left[\frac{\partial v_2(\omega)}{\partial\omega}\right]_{\omega=\varepsilon_a-\varepsilon_A}\Bigg\}+O(\alpha^4). \tag{49}$$

The term $v_1(\varepsilon_a-\varepsilon_A)$ gives the contribution of the one-photon exchange graph of Fig. 1. The term $v_2(\varepsilon_a-\varepsilon_A)$ presents the contribution of the two-photon exchange graphs of Fig. 2. This term includes also the reference-state part of these graphs. The term $v_3(\varepsilon_a-\varepsilon_A)$ gives the contribution of the three-photon exchange graph of Fig. 3. Here this term does not include the contribution of the reference states because we consider the three-photon exchange in the framework of RMBPT. The term with a derivative in Eq. (49), as the term with a derivative in Eq. (44), does not correspond to any certain graphs. As in the case of Eq. (44), it is again connected with the reducible (reference-state) contribution of the graphs in Fig. 3.

It should be stressed that if we were to include in the LPA also the first- and second-order radiative corrections as well as screened radiative corrections, we should use for $v_1(\omega)$ the sum of Eqs. (34) and (45) and a vacuum polarization part. For $v_2(\omega)$, we should use the sum of Eqs. (41) and (46) plus all the contributions for second-order radiative corrections and screened corrections. Then instead of the formula (49), we would have

$$\omega^{\mathrm{res}}=\varepsilon_a-\varepsilon_A+\mathrm{Re}\Bigg\{v_1(\varepsilon_a-\varepsilon_A)+v_2(\varepsilon_a-\varepsilon_A)+v_1(\varepsilon_a-\varepsilon_A)\times\left[\frac{\partial v_1(\omega)}{\partial\omega}\right]_{\omega=\varepsilon_a-\varepsilon_A}+v_3(\varepsilon_a-\varepsilon_A)+\frac{1}{2}v_1(\varepsilon_a-\varepsilon_A)^2\times\left[\frac{\partial^2 v_1(\omega)}{\partial\omega^2}\right]_{\omega=\varepsilon_a-\varepsilon_A}+v_1(\varepsilon_a-\varepsilon_A)\left[\frac{\partial v_1(\omega)}{\partial\omega}\right]^2_{\omega=\varepsilon_a-\varepsilon_A}+v_1(\varepsilon_a-\varepsilon_A)\left[\frac{\partial v_2(\omega)}{\partial\omega}\right]_{\omega=\varepsilon_a-\varepsilon_A}+v_2(\varepsilon_a-\varepsilon_A)\times\left[\frac{\partial v_1(\omega)}{\partial\omega}\right]_{\omega=\varepsilon_a-\varepsilon_A}\Bigg\}+O(\alpha^4). \tag{50}$$

Note that the presence of the derivatives $[\partial v_1(\omega)/\partial\omega]$ does not distort the Lorentz line shape while the term $[\partial^2 v_1(\omega)/\partial\omega^2]$ leads to a small distortion [50].

Finally, if we were to extend the LPA for the three-electron case, we would get the same formulas (49) and (50) where the functions $v_2(\omega)$ and $v_3(\omega)$ should contain also the contribution of the three-electron graphs of Figs. 4 and 5.

VI. REDUCIBLE CONTRIBUTIONS TO THE INTERELECTRON INTERACTION IN TWO- AND THREE-ELECTRON IONS

From the derivations in the preceding section, we obtain the following expression for the ''box'' reducible contribution in two-electron atoms:

$$F^{(2)(\mathrm{box,red})}_{a'b'ab}=-\frac{1}{2}\sum_{gg'}\sum_{n_1n_2}{}''\Bigg\{\frac{i}{2\pi}\int_{-\infty}^{\infty}\frac{I^g(\Omega)_{a'b'n_1n_2}I^{g'}(\Omega-\varepsilon_{a'}+\varepsilon_a)_{n_1n_2ab}}{(\Omega-\varepsilon_{n_2}+\varepsilon_{b'}+i0\varepsilon_{n_2})^2}d\Omega+\frac{i}{2\pi}\int_{-\infty}^{\infty}\frac{I^g(\Omega)_{b'a'n_1n_2}I^{g'}(\Omega-\varepsilon_a+\varepsilon_{a'})_{n_1n_2ba}}{(\Omega-\varepsilon_{n_2}+\varepsilon_{a'}+i0\varepsilon_{n_2})^2}d\Omega\Bigg\}, \tag{51}$$

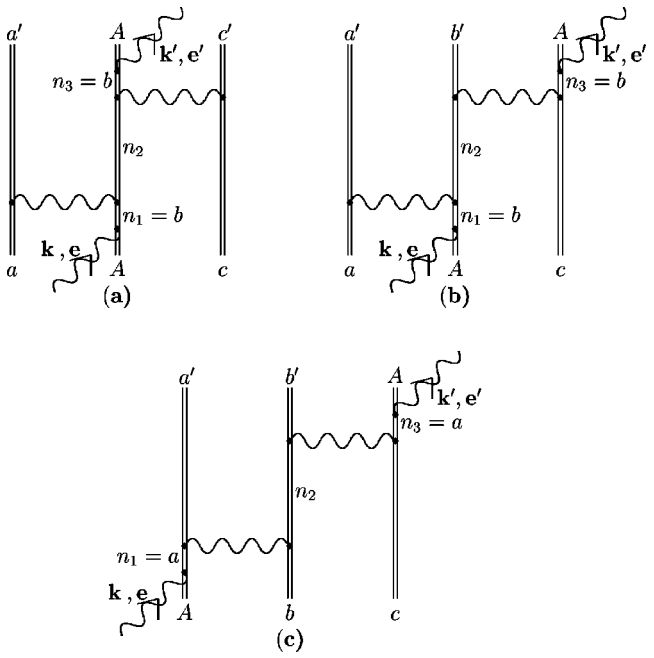

FIG. 10. The second-order interelectron interaction correction to the scattering amplitude in the resonance approximation for three-electron ions.

where the double dash indicates that the summation runs over states which are not included in the summation in Eq. (24). The ''cross'' reducible corrections can be obtained in the same way as the ''box'' corrections, though, in principle, they can be derived also in a simpler way directly by formulas (12) and (13). The corresponding expression is given by

TABLE I. Different contributions to the second-order interelectron interaction for a two-electron configuration $1s_{1/2}2s_{1/2}\,{}^1S_0$ (eV). The numbers in the table present the ionization energy of the $2s_{1/2}$ electron with the opposite sign.

Contribution	$Z=30$	70	80	92
Coulomb-Coulomb				
$\Delta E^{\mathrm{box,irr}}$	−3.290	−4.317	−4.845	−5.768
$\Delta E^{\mathrm{cross,irr}}$	0.003	0.030	0.046	0.074
ΔE(total)	−3.287	−4.286	−4.799	−5.695
Coulomb-Breit				
$\Delta E^{\mathrm{box,irr}}$	−0.277	−1.702	−2.375	−3.499
$\Delta E^{\mathrm{box,red}}$	0.103	0.724	1.038	1.569
$\Delta E^{\mathrm{cross,irr}}$	0.002	−0.088	−0.108	−0.140
$\Delta E^{\mathrm{cross,red}}$	−0.006	−0.517	−0.147	−0.242
ΔE(total)	−0.179	−1.159	−1.592	−2.312
Breit-Breit				
$\Delta E^{\mathrm{box,irr}}$	−0.010	−0.179	−0.302	−0.524
$\Delta E^{\mathrm{box,red}}$	0.002	0.071	0.127	0.239
$\Delta E^{\mathrm{cross,irr}}$	0.000	0.032	0.056	0.096
$\Delta E^{\mathrm{cross,red}}$	0.000	0.003	0.007	0.014
ΔE(total)	−0.008	−0.073	−0.113	−0.178
Total				
ΔE	−3.473	−5.519	−6.504	−8.184

TABLE II. Different contributions to the third-order interelectron interaction for a two-electron configuration $1s_{1/2}2s_{1/2}\,{}^1S_0$ (eV). The numbers in the table present the ionization energy of the $2s_{1/2}$ electron with the opposite sign.

Contribution	$Z=30$	70	80	92
Coulomb-Coulomb-Coulomb	0.010	0.007	0.012	0.016
Coulomb-Coulomb-Breit	0.006	0.015	0.016	0.022
Coulomb-Breit-Breit	0.001	0.006	0.008	0.012
Breit-Breit-Breit	0.000	0.000	0.002	0.002
Total ΔE	0.017	0.029	0.038	0.052

$$F^{(2)(\mathrm{cross,irr})}_{a'b'ab} = \sum_{gg'} \sum_{n_1 n_2}{}'' \frac{i}{2\pi} \times \int_{-\infty}^{\infty} \frac{I^g(\Omega)_{b'n_2n_1a} I^{g'}(\Omega-\varepsilon_{a'}+\varepsilon_a)_{n_1a'bn_2}}{(\Omega-\varepsilon_{n_2}+\varepsilon_a+i0\varepsilon_{n_2})^2} d\Omega, \tag{52}$$

where the summation runs over the states which are not included in the summation in Eq. (25). The contributions of ''box'' and ''cross'' graphs for two-electron ions are definedby Eq. (20). From Eqs. (51) and (52), it follows automatically that the corrections vanish for $g=g'=c$.

For the ''box'' and ''cross'' reducible contributions in three-electron ions, Eq. (27) holds. So it remains to consider

TABLE III. Different contributions to the second-order interelectron interaction for a two-electron configuration $1s_{1/2}2s_{1/2}\,{}^3S_1$ (eV). The numbers in the table present the ionization energy of the $2s_{1/2}$ electron with the opposite sign.

Contribution	$Z=30$	70	80	92
Coulomb−Coulomb				
$\Delta E^{\mathrm{box,irr}}$	−1.345	−1.643	−1.785	−2.017
$\Delta E^{\mathrm{cross,irr}}$	0.000	0.003	0.005	0.009
ΔE(total)	−1.345	−1.641	−1.780	−2.009
Coulomb-Breit				
$\Delta E^{\mathrm{box,irr}}$	−0.002	−0.008	−0.010	−0.012
$\Delta E^{\mathrm{box,red}}$	−0.000	−0.004	−0.006	−0.011
$\Delta E^{\mathrm{cross,irr}}$	−0.001	−0.005	−0.009	−0.015
$\Delta E^{\mathrm{cross,red}}$	0.000	0.001	0.002	0.004
ΔE(total)	−0.003	−0.016	−0.024	−0.033
Breit-Breit				
$\Delta E^{\mathrm{box,irr}}$	−0.000	0.003	0.004	0.005
$\Delta E^{\mathrm{box,red}}$	0.000	0.000	0.000	0.000
$\Delta E^{\mathrm{cross,irr}}$	−0.001	0.007	0.011	0.018
$\Delta E^{\mathrm{cross,red}}$	0.000	0.000	0.001	0.002
ΔE(total)	−0.001	0.010	0.016	0.024
Total				
ΔE	−1.348	−1.647	−1.789	−2.018

TABLE IV. Different contributions to the third-order interelectron interaction for a two-electron configuration $1s_{1/2}2s_{1/2}\,{}^3S_1$ (eV). The numbers in the table present the ionization energy of the $2s_{1/2}$ electron with the opposite sign.

Contribution	$Z=30$	70	80	92
Coulomb-Coulomb-Coulomb	−0.004	−0.001	−0.001	0.000
Coulomb-Coulomb-Breit	0.000	0.001	0.001	0.001
Coulomb-Breit-Breit	0.000	0.000	0.000	0.000
Breit-Breit-Breit	0.000	0.000	0.000	0.000
Total ΔE	−0.004	0.000	0.000	0.001

the reducible ''step'' contributions for three-electron ions. In principle, this contribution is simpler than the ''box'' one and hence the adiabatic formula (11) can be applied. However, the line profile approach is also applicable in this case and we will demonstrate how it works. To employ this approach, we have to consider the Feynman graph for the scattering amplitude depicted in Fig. 10.

The ''step'' reducible contribution to the three-electron atom is

$$F^{(2)(\mathrm{step,red})}_{a'b'c'abc}=\sum_{gg'}\sum_{n}{}''\ \frac{\partial}{\partial\omega}I^{g}(\varepsilon_a-\varepsilon_{a'}+\omega)_{na'ba}\times I^{g'}(\varepsilon_{c'}-\varepsilon_c+\omega)_{b'c'nc}\big|_{\omega=0}, \tag{53}$$

where the summation runs over the states which are not included in the summation in Eq. (29).

The formula for the reducible part of the third-order Coulomb and unretarded Breit ''box'' corrections can be expressed as

$$F^{(3)(\mathrm{box,red})}_{a'b'ab}=\sum_{gg'g''}\sum_{n_1n_2n_3n_4}{}''\ I^{g}_{a'b'n_3n_4}I^{g'}_{n_3n_4n_1n_2}I^{g''}_{n_1n_2ab}\times\left\{\frac{(-1)}{2(\varepsilon_{n_3}+\varepsilon_{n_4}-\varepsilon_{a'}-\varepsilon_{b'})^2}+\frac{(-1)}{2(\varepsilon_{n_1}+\varepsilon_{n_2}-\varepsilon_{a}-\varepsilon_{b})^2}\right\}, \tag{54}$$

where the double dash indicates that the summation is running only over the reference states. The terms with zero denominators in Eq. (54) should be omitted. The third-order ''step-box'' reducible corrections (see Fig. 5) are given by the formula

TABLE V. The different contributions to the total energy of the two-electron configuration $1s_{1/2}2s_{1/2}\,{}^1S_0$ (eV). The numbers in the table present the ionization energy of the $2s_{1/2}$ electron with the opposite sign.

Contribution	$Z=30$	70	80	92	Ref.
Zero-order	−3108.3209	−18250.3701	−24622.1720	−34215.4976	TW[a]
Nuclear size (NS)	0.0145(5)	3.10(5)	9.34(14)	37.76(6)	TW
First-order interelectron interaction	196.0797(5)	542.484(5)	665.38(1)	850.116(5)	TW
Second-order interelectron interaction	−3.758(3)	−5.519(3)	−6.504(3)	−8.184(3)	TW
Third-order interelectron interaction	0.017(1)	0.029(3)	0.038(4)	0.052(5)	TW
SE with NS	0.9674	20.5890	35.3911	65.4183	[58,59]
VP with NS	−0.0834	−3.419(1)	−6.900(2)	−15.658(3)	[57,60]
Recoil	0.0269	0.0674	0.0870	0.1279	[61]
Total	−2915.057(4)	−17693.04(6)	−23925.34(16)	−33285.87(8)	TW
AO	−2914.8875	−17693.7864	−23926.3243	−33288.4601	[25]
UT	−2914.8326	−17692.9476	−23924.7251	−33284.7190	[62]

[a]TW, this work.

TABLE VI. The different contributions to the total energy of the two-electron configuration $1s_{1/2}2s_{1/2}\,{}^3S_1$ (eV). The numbers in the table present the ionization energy of the $2s_{1/2}$ electron with the opposite sign.

Contribution	$Z=30$	70	80	92	Ref.
Zero-order	−3108.3209	−18250.3701	−24622.1720	−34215.4976	TW
Nuclear size (NS)	0.0145(5)	3.10(5)	9.34(14)	37.76(6)	TW
First-order interelectron interaction	156.5068(5)	402.905(5)	480.13(1)	588.169(5)	TW
Second-order interelectron	−1.348(3)	−1.647(3)	−1.789(3)	−2.018(3)	TW
interaction	−1.3483	−1.6548	−1.7956	−2.0203	[30]
Third-order interelectron interaction	−0.004(1)	0.000(1)	0.000(1)	0.001(1)	TW
SE with NS	0.96737	20.5890	35.3911	65.4183	[58,59]
VP with NS	−0.0834	−3.419(1)	−6.900(2)	−15.658(3)	[57,60]
Recoil	0.0269	0.0674	0.0870	0.1279	[61]
Total	−2952.241(5)	−17828.78(6)	−24105.91(15)	−33541.70(7)	TW
AO	−2952.3165	−17829.3421	−24106.6213	−33543.8853	[25]
UT	−2952.2890	−17829.1872	−24106.3346	−33543.1669	[62]

TABLE VII. Different contributions to the second-order interelectron interaction for a three-electron configuration $(1s)^2 2p_{1/2}$ (eV). The numbers in the table present the ionization energy of the $2p_{1/2}$ electron with the opposite sign.

Contribution	$Z=30$	70	80	92
Coulomb-Coulomb				
$\Delta E^{\mathrm{box,irr}}$	−12.284	−8.551	−9.312	−10.968
$\Delta E^{\mathrm{cross,irr}}$	0.001	0.024	0.043	0.082
$\Delta E^{\mathrm{step,irr}}$	1.478	−6.513	−7.985	−10.309
ΔE(total)	−10.804	−15.040	−17.254	−21.195
Coulomb-Breit				
$\Delta E^{\mathrm{box,irr}}$	0.843	−0.132	−0.619	−1.447
$\Delta E^{\mathrm{box,red}}$	0.004	0.035	0.051	0.081
$\Delta E^{\mathrm{cross,irr}}$	−0.006	−0.044	−0.060	−0.078
$\Delta E^{\mathrm{cross,red}}$	−0.008	−0.071	−0.105	−0.166
$\Delta E^{\mathrm{step,irr}}$	−1.220	−2.088	−2.524	−3.269
$\Delta E^{\mathrm{step,red}}$	−0.016	−0.114	−0.173	−0.291
ΔE(total)	−0.403	−2.414	−3.430	−5.170
Breit-Breit				
$\Delta E^{\mathrm{box,irr}}$	−0.038	−0.184	−0.389	−0.585
$\Delta E^{\mathrm{box,red}}$	0.000	0.003	0.005	0.012
$\Delta E^{\mathrm{cross,irr}}$	0.001	0.031	0.056	0.112
$\Delta E^{\mathrm{cross,red}}$	0.000	0.004	0.009	0.018
$\Delta E^{\mathrm{step,irr}}$	0.037	0.145	0.168	0.191
$\Delta E^{\mathrm{step,red}}$	0.000	0.005	0.009	0.014
ΔE(total)	0.001	0.004	−0.143	−0.237
Total				
ΔE	−11.206	−17.450	−20.827	−26.602

$$F^{(3)(\text{step-box,red})}_{a'b'c'abc} = \sum_{gg'g''} \sum_{n_1n_2n_3}{}'' \; I^{g}_{a'b'n_1n_3} I^{g'}_{n_3c'n_2c} I^{g''}_{n_1n_2ab} \left\{ \frac{(-1)}{2(\varepsilon_{n_1}+\varepsilon_{n_3}-\varepsilon_{a'}-\varepsilon_{b'})^2} + \frac{(-1)}{2(\varepsilon_{n_1}+\varepsilon_{n_2}-\varepsilon_{a}-\varepsilon_{b})^2} \right\}$$

$$+2 \sum_{n_1n_2n_3}{}'' \; I^{g}_{b'c'n_3c} I^{g'}_{a'n_3n_1n_2} I^{g''}_{n_1n_2ab} \left\{ \frac{(-1)}{2(\varepsilon_{n_1}+\varepsilon_{n_2}-\varepsilon_{a}-\varepsilon_{b})^2} + \frac{(-1)}{2(\varepsilon_{n_3}+\varepsilon_{a'}-\varepsilon_{a}-\varepsilon_{b})^2} \right\}$$

$$+ \sum_{n_1n_2n_3}{}'' \; I^{g}_{a'c'n_1n_3} I^{g'}_{b'n_3n_2c} I^{g''}_{n_1n_2ab} \left\{ \frac{(-1)}{2(\varepsilon_{n_1}+\varepsilon_{n_2}-\varepsilon_{a}-\varepsilon_{b})^2} + \frac{(-1)}{2(\varepsilon_{n_1}+\varepsilon_{n_3}-\varepsilon_{a'}-\varepsilon_{c'})^2} \right\}, \tag{55}$$

where the first summation runs over the states for which either the set $\{n_1,n_2,c\}$ or the set $\{n_1,n_3,c'\}$ are equivalent to the set $\{a,b,c\}$, the second summation runs over the states for which the sets $\{n_1,n_2,c\}$ or $\{a',n_3,c\}$ are equivalent to the set $\{a,b,c\}$, and the third summation does not run over the states for which the sets $\{n_1,n_2,c\}$ or $\{n_1,n_3,b'\}$ are equivalent to the set $\{a,b,c\}$ (the reference-state cases).

VII. RESULTS AND DISCUSSION

The results of the calculations for two-electron ions are given in Tables I–VI. In Tables I and III, the different contributions to the second-order interaction for the configurations $1s_{1/2}2s_{1/2}\ {}^1S_0$ and $1s_{1/2}2s_{1/2}\ {}^3S_1$ are listed. In Tables V and VI, the total energies of the two-electron configurations are given in comparison with other calculations. The zero-order values in Tables V and VI correspond to the Sommerfeld binding energy for the $2s_{1/2}$ electron. Nuclear size corrections are calculated in this work with the Fermi distribution for the nuclear charge. We solved the Dirac equation with the potential that originates from a Fermi nuclear density distribution

$$\rho(r) = \frac{N}{1+\exp[(r-c)/a]}, \tag{56}$$

where N is the normalization constant and which is defined by

$$4\pi \int_0^\infty \rho(r) r^2 \, dr = eZ. \tag{57}$$

The parameter $a = 0.5350$ fm and c is defined from the condition

$$4\pi \int_0^\infty \rho(r) r^4 \, dr = \langle r^2 \rangle, \tag{58}$$

where $\langle r^2 \rangle^{1/2}$ is the root-mean-square nuclear radius. The interelectron interaction corrections were also calculated in this work for extended nuclei. In order to calculate zero- and first-order corrections with higher accuracy, we took the values for $\langle r^2 \rangle^{1/2}$ and the corresponding estimates for the accuracy from [20]. For the second- and third-order corrections, we used the empirical expression [57]

$$\langle r^2 \rangle^{1/2} = (0.836A^{1/3} + 0.570) \text{ fm}, \tag{59}$$

where A is the atomic number.

The electron self-energy (SE) correction with the nuclear size taken into account was taken from [58] and [59], and the vacuum polarization (VP) correction was from [57] and [60]. For the recoil correction, we used the data given in [61]. There are no screening corrections to SE and VP in the literature, evaluated directly for the two-electron configurations. So we omitted these corrections in Tables V and VI. The total result is compared with the relativistic all-order theory (AO) [25] and the unified theory (UT) [62]. Compared to the QED approach, these theories are missing (i) negative energy states, (ii) crossed photons contribution, and (iii) exact retardation effects. AO takes partly into account retardation and higher-order interelectron interactions. UT starts from the nonrelativistic Schrödinger equation and takes into account accurately interelectron interaction. However, relativistic and QED effects are considered only approximately.

In this paper in the framework of the RMBPT based on the Coulomb functions, we calculated also the third order of

TABLE VIII. Different contributions to the third-order interelectron interaction for a three-electron configuration $(1s)^2 2p_{1/2}$ (eV). The numbers in the table present the ionization energy of the $2p_{1/2}$ electron with the opposite sign.

Contribution	$Z=30$	70	80	92
Coulomb-Coulomb-Coulomb	−0.061	0.019	0.041	0.083
Coulomb-Coulomb-Breit	0.019	0.059	0.084	0.119
Coulomb-Breit-Breit	−0.030	0.012	0.017	0.031
Breit-Breit-Breit	0.000	0.000	0.002	0.000
Total ΔE	−0.072	0.090	0.144	0.233

TABLE IX. Different contributions to the second-order interelectron interaction for a three-electron configuration $(1s)^2 2s_{1/2}$ (eV). The numbers in the table present the ionization energy of the $2s_{1/2}$ electron with the opposite sign.

Contribution	$Z=30$	70	80	92
Coulomb-Coulomb				
$\Delta E^{\mathrm{box,irr}}$	−3.662	−4.623	−5.100	−5.910
$\Delta E^{\mathrm{cross,irr}}$	0.002	0.019	0.030	0.050
$\Delta E^{\mathrm{step,irr}}$	−3.490	−4.370	−4.802	−5.526
ΔE(total)	−7.150	−8.975	−9.872	−11.386
Coulomb-Breit				
$\Delta E^{\mathrm{box,irr}}$	−0.141	−0.863	−1.202	−1.771
$\Delta E^{\mathrm{box,red}}$	0.051	0.356	0.509	0.768
$\Delta E^{\mathrm{cross,irr}}$	0.001	−0.052	−0.069	−0.092
$\Delta E^{\mathrm{cross,red}}$	−0.003	−0.045	−0.071	−0.115
$\Delta E^{\mathrm{step,irr}}$	−0.040	−0.242	−0.330	−0.465
$\Delta E^{\mathrm{step,red}}$	−0.008	−0.063	−0.094	−0.149
ΔE(total)	−0.140	−0.909	−1.256	−1.824
Breit-Breit				
$\Delta E^{\mathrm{box,irr}}$	−0.005	−0.088	−0.143	−0.253
$\Delta E^{\mathrm{box,red}}$	0.001	0.035	0.064	0.120
$\Delta E^{\mathrm{cross,irr}}$	−0.002	0.027	0.044	0.075
$\Delta E^{\mathrm{cross,red}}$	0.000	0.002	0.004	0.009
$\Delta E^{\mathrm{step,irr}}$	0.001	0.015	0.027	0.052
$\Delta E^{\mathrm{step,red}}$	−0.001	−0.006	−0.010	−0.020
ΔE(total)	−0.005	−0.014	−0.015	−0.017
Total				
ΔE	−7.295	−9.898	−11.143	−13.228

the interelectron interaction. The results are given in Tables II and IV. For these data, we give 10% inaccuracy. This estimate follows from [27], where the comparison was made between QED and RMBPT calculations for the $(1s_{1/2})^2$ configuration of He-like ions with $Z=92$. Since the fourth-order interelectron interaction is approximately Z times smaller than the third-order interaction, we can assume that the higher-order contributions are smaller than the third-order inaccuracy.

In Tables VII, VIII, IX and X, the different contributions to the second-order interaction for the three-electron configurations $(1s)^2 2s_{1/2}$ and $(1s)^2 2p_{1/2}$ are listed and the different contributions to total energies of the three-electron configurations are provided in comparison with other calculations in Tables XI and XII.

In Table XIII, we give the different contributions to the splitting $2p_{1/2}$-$2s_{1/2}$ in Li-like uranium. The full set of the second-order radiative correction is not known for $2s_{1/2}$ and $2p_{1/2}$ states. The unknown corrections are second-order self-energy corrections. For the ground state of H-like U, the values for these corrections were reported recently in [63]. Evaluating the ratio of these corrections to the loop-after-loop correction [Fig. 7(b)] for the ground state $r=-1.28/0.97$, assuming that this ratio is approximately the same for the $2s_{1/2}$ state, using the known value for the loop-after-loop correction for $2s_{1/2}$ [64], and neglecting the contribution of the $2p_{1/2}$ state [65], we obtain the estimate given in Table XIII. We assume the inaccuracy of such a rough estimate to be as high as 100%. Finally, in Table XIV the different theoretical and experimental data for $2p_{1/2}$-$2s_{1/2}$

TABLE X. Different contributions to the third-order interelectron interaction for a three-electron configuration $(1s)^2 2s_{1/2}$ (eV). The numbers in the table present the ionization energy of the $2s_{1/2}$ electron with the opposite sign.

Contribution	$Z=30$	70	80	92
Coulomb-Coulomb-Coulomb	−0.017	0.007	0.015	0.026
Coulomb-Coulomb-Breit	0.005	0.018	0.021	0.029
Coulomb-Breit-Breit	0.000	0.004	0.005	0.012
Breit-Breit-Breit	0.000	−0.001	0.001	0.001
Total ΔE	−0.012	0.028	0.042	0.068

TABLE XI. The different contributions to the total energy of the three-electron configuration $(1s)^2 2p_{1/2}$ (eV). The numbers in the table present the ionization energy of the $2p_{1/2}$ electron with the opposite sign.

Contribution	$Z=30$	70	80	92	Ref.
Zero-order	−3108.3209	−18250.3701	−24622.1720	−34215.4976	TW
Nuclear size (NS)	0.0001	0.18(5)	0.75(14)	4.42(6)	TW
First-order interelectron interaction	394.9471(5)	1078.213(5)	1317.19(1)	1676.142(5)	TW
Second-order interelectron	−11.206(3)	−17.450(3)	−20.827(3)	−26.602(3)	TW
interaction	−11.186(5)	−17.546(5)	−20.828(5)	−26.597(5)	[28,29,67]
Third-order interelectron	−0.072(7)	0.090(9)	0.144(14)	0.233(23)	TW
interaction (RMBPT)	−0.047(15)	0.086(45)	0.131(65)	0.209(100)	[66]
SE with NS	−0.0219	1.1371	3.2341	9.5504	[58,59]
VP with NS	−0.0011	−0.297(1)	−0.831(2)	−2.704(3)	[57,60]
SE screening	−0.0283	−0.4977	−0.9305	−1.9774	[20]
VP screening	0.0031	0.0948	0.2034	0.5216	[19]
Recoil	0.0106	0.0295	0.0386	0.0560	[61]
Nuclear polarization				−0.0039(10)	[70]
Total	−2724.68(1)	−17188.87(7)	−23323.20(15)	−32555.86(7)	TW
RMBPT	−2724.5877			−32561.2268	[22]

splitting are presented.

Comparing our results with the other calculations known for $1s_{1/2}2s_{1/2}\,^1S_0$ and $1s_{1/2}2s_{1/2}\,^3S_1$ states of He-like ions, we find that the full QED evaluation of the two-photon exchange for $1s_{1/2}2s_{1/2}\,^3S_1$ states in [30] deviates from our results for all Z values not more than by 0.0003 a.u. Our numerical procedure should give an error less then 10^{-4} a.u. The three-photon QED exchange was not taken into account in [30]. The details of the numerical procedure and accuracy estimates are given in Appendix B.

TABLE XII. The different contributions to the total energy of the three-electron configuration $(1s)^2 2s_{1/2}$ (eV). The numbers in the table present the ionization energy of the $2s_{1/2}$ electron with the opposite sign.

Contribution	$Z=30$	70	80	92	Ref.
Zero-order	−3108.3209	−18250.3701	−24622.1720	−34215.4976	TW
Nuclear size (NS)	0.0145(5)	3.10(5)	9.34(14)	37.76(6)	TW
First-order interelectron interaction	332.7995(5)	875.600(5)	1052.88(1)	1307.310(5)	TW
Second-order interelectron	−7.295(3)	−9.898(3)	−11.143(3)	−13.228(3)	TW
interaction	−7.297	−9.899(5)	−11.147(5)	−13.226(5)	[28,29,67]
Third-order interelectron	−0.012(1)	0.028(3)	0.042(4)	0.068(7)	TW
interaction (RMBPT)	−0.011(7)	0.039(20)	0.055(28)	0.078(40)	[66]
SE with NS	0.9674	20.5890	35.3911	65.4183	[58,59]
VP with NS	−0.0834	−3.419(1)	−6.900(2)	−15.658(3)	[57,60]
SE screening	−0.1282	−1.3158	−2.0627	−3.5017	[20]
VP screening	0.0109	0.2249	0.4182	0.8815	[19]
Recoil	0.0269	0.0674	0.0870	0.1279	[61]
Nuclear polarization				−0.0377(94)	[70]
Total	−2782.020(5)	−17365.39(6)	−23544.12(15)	−32836.36(8)	TW
RMBPT	−2782.7867			−32884.3689	[22]

TABLE XIII. Different contributions to the splitting $2p_{1/2}$-$2s_{1/2}$ in Li-like uranium.

Correction		Numerical value (eV)	Reference
Nuclear finite size correction to the binding energy		−33.35(6)	[71]
Interelectron interaction	first order	368.83	This work
QED-INT	second order	−13.37	This work
		−13.37	[28]
	third order	0.17(2)	This work
		0.14(7)	[28]
Electron self-energy including nuclear size correction (SE)		−55.87	[59]
Vacuum polarization including nuclear size correction (VP)		12.94	[72]
Electron self-energy screening		1.52	[20]
Vacuum polarization screening		−0.36	[19]
Second-order radiative corrections	SESE[a]	0.10	[64]
	SESE[b]	−0.13(13)	Estimate, TW
	VPVP	0.13	[65]
	SEVP	−0.21	[65]
Nuclear recoil		−0.07	[61]
Nuclear polarization		0.03	[73]
Total theory	QED	280.36(21)	This work
	QED	280.44(20)	[28]
	RMBPT	280.54(15)	[16]
Experiment		280.59(9)	[9]

[a]Loop after loop, irreducible.

[b]Loop after loop reducible and other SESE.

In the tables, in which only the data calculated in this work are presented, the error is not indicated. It is clear that rounding off numbers provides a certain error. So in the tables containing a large number of contributions, the total values may differ slightly from the sum of the contributions due to this rounding off.

The full QED evaluation of the two-photon exchange and the approximate QED evaluation of three-photon exchange for the state $1s_{1/2}2s_{1/2}\,{}^1S_0$ are done for the first time to our knowledge in our paper. The disagreement of the total energy of $1s_{1/2}2s_{1/2}\,{}^1S_0$ and $1s_{1/2}2s_{1/2}\,{}^3S_1$ states with the earlier AO and UT calculations is about $1-2$ eV. This may be caused by the absence of the SE and VP screening corrections, not yet calculated in the QED framework. Approximately these corrections were taken into account in UT and AO methods. The evaluation of the two-photon exchange for the three-electron configurations $(1s)^2 2s_{1/2}$ and $(1s)^2 2p_{1/2}$ coincides with earlier calculations in [28] at least within four digits for the values $Z=80$ and 92 calculated in [28]. The three-photon exchange corrections for the same configurations made in the framework of the RMBPT coincide with the results given in [66] within the quoted error bars. Note that in [66] only one Breit interaction was taken into account. In our work, we considered one, two, and three Breit interactions. As follows from Tables VIII and X, the contribution of the Coulomb-Breit-Breit interaction graphs is comparable with the contributions of the Coulomb-Coulomb-Coulomb and Coulomb-Coulomb-Breit graphs. It should be mentioned that as follows from Tables VIII, X, and XIV, omitting the two and three Breit photons within RMBPT yields a better agreement

TABLE XIV. Different theoretical and experimental data for the $2p_{1/2}$-$2s_{1/2}$ splitting in Li-like ions.

Z	This work	Blundell Ref. [74]	Kim *et al.* Ref. [75]	Yerokhin *et al.* Ref. [67]	Experiment	
30	57.34(1)	57.389(2)	57.381	57.384(4)	57.384(3)	Staude *et al.*, Ref. [76]
70	176.52(7)	176.56(2)	176.567	176.44(6)		
80	220.92(15)	220.99(3)	221.028	220.93(15)		
92	280.36(21)	280.83(10)	280.677	280.44(20)	280.59(9)	Schweppe *et al.*, Ref. [9]

with experiment, for example for $Z=30$ [67]. However, this means only that in these cases the QED interaction beyond RMBPT should be taken into account precisely.

For the configuration $(1s)^2 2s_{1/2}$, our total energy differs from the value obtained in [22] by 48 eV. In [22], the RMBPT approach based on zero-order Hartree-Fock functions was employed. However, our results for the splitting $2p_{1/2}$-$2s_{1/2}$ in Li-like uranium agree well with experimental data and with other theoretical values.

ACKNOWLEDGMENTS

The authors are indebted to V. M. Shabaev and V. A. Yerokhin for clarifying discussions and for their information on their own investigations on the subject. O.A. is grateful to the Technische Universität Dresden for the hospitality during his visit in 2000 and to the DFG for financial support. The work of O.A. and L.N. was supported by RFBR Grant No. 99-02-18526. G.P. and G.S. acknowledge financial support from BMBF, and GSI.

APPENDIX A

The irreducible *S*-matrix elements in Eq. (11) can be defined as the matrix elements that cannot be reduced to the products of two or more matrix elements of the type $\langle\Phi_a|\cdots|\Phi_a\rangle$. Thus in Eq. (11) only the first terms in each set of square brackets could be irreducible. However, in these terms the reducible parts can also arise.

Thus for the evaluation of the irreducible contribution instead of Eqs. (10) and (11) one can use the formula

$$\Delta E_a^{(n),\mathrm{irr}} = \lim_{\lambda\to 0} \frac{in\lambda}{2} \langle\Phi_a|\hat{S}_\lambda^{(n)}|\Phi_a\rangle_{\mathrm{irr}}. \tag{A1}$$

In Eq. (A1), the limit $\lambda\to 0$ can be done explicitly. For this purpose we use the adiabatic *S*-matrix expression (8):

$$\hat{S}_\lambda^{(n)}(\infty,-\infty) = (-i)^n e^n \int_{-\infty}^{\infty} \hat{H}_{\mathrm{int}}(t_1) e^{-\lambda|t_1|} dt_1 \int_{-\infty}^{t_1} \hat{H}_{\mathrm{int}}(t_2) \times e^{-\lambda|t_2|} dt_2 \cdots \int_{-\infty}^{t_{n-1}} \hat{H}_{\mathrm{int}}(t_n) e^{-\lambda|t_n|} dt_n . \tag{A2}$$

Acting by the operator $\hat{S}_\lambda^{(n)}(\infty,-\infty)$ on the state vector $|\Phi_a\rangle$ and integrating over t_n, we obtain

$$\begin{aligned}
&\int_{-\infty}^{t_{n-1}} \hat{H}_{\mathrm{int}}(t_n) e^{-\lambda|t_n|} dt_n |\Phi_a\rangle \\
&= \int_{-\infty}^{t_{n-1}} e^{i(\hat{H}_0-\varepsilon_a)t_n - \lambda|t_n|} dt_n \hat{H}_{\mathrm{int}}|\Phi_a\rangle \\
&= e^{i(\hat{H}_0-\varepsilon_a)t_{n-1} - \lambda|t_{n-1}|} \frac{1}{i(\hat{H}_0-\varepsilon_a)} \hat{H}_{\mathrm{int}}|\Phi_a\rangle .
\end{aligned} \tag{A3}$$

Here we took into account that for the reducible contribution, the denominator in Eq. (A3) cannot be equal to zero and therefore it is possible to put $\lambda=0$ in this denominator. Continuing the integration over time variables, we obtain

$$\langle\Phi_a|\hat{S}_\lambda^{(n)}|\Phi_a\rangle_{\mathrm{irr}} = -ie^n \langle\Phi_a| \int_{-\infty}^{\infty} e^{-i(\varepsilon_a-\hat{H}_0)t_1 - n\lambda|t_1|} dt_1 \hat{H}_{\mathrm{int}} \times \left(\frac{1}{\varepsilon_a-\hat{H}_0}\hat{H}_{\mathrm{int}}\right)^{n-1} |\Phi_a\rangle_{\mathrm{irr}}. \tag{A4}$$

The last integration over t_1 yields

$$\langle\Phi_a|\hat{S}_\lambda^{(n)}|\Phi_a\rangle_{\mathrm{irr}} = -\frac{2i}{n\lambda} \langle\Phi_a|\hat{H}_{\mathrm{int}} \left(\frac{1}{\varepsilon_a-\hat{H}_0}\hat{H}_{\mathrm{int}}\right)^{n-1} |\Phi_a\rangle_{\mathrm{irr}}. \tag{A5}$$

Here all the operators are written in Schrödinger representation. Inserting Eq. (A5) into Eq. (A1), we have

$$\Delta E_{\mathrm{irr}}^{(n)} = e^n \langle\Phi_a|\hat{H}_{\mathrm{int}} \left(\frac{1}{\varepsilon_a-\hat{H}_0}\hat{H}_{\mathrm{int}}\right)^{n-1} |\Phi_a\rangle_{\mathrm{irr}}. \tag{A6}$$

In Eq. (A6), the limit $\lambda\to 0$ is already done.

Now we will evaluate the energy shift $\Delta E_{\mathrm{irr}}^{(n)}$ in another way. Consider the irreducible part of the nondiagonal matrix element of the operator $\hat{S}_\lambda^{(n)}(\infty,-\infty)$ between two different states Φ_a and Φ_b with different energies ε_a and ε_b. Then we can repeat all the integrations over $t_2, \ldots, t_{n-1}$ as before and only the last integration over t_1 will be different:

$$\begin{aligned}
\lim_{\lambda\to 0}\langle\Phi_b|\hat{S}_\lambda^{(n)}|\Phi_a\rangle_{\mathrm{irr}} &= -i\langle\Phi_b| \int_{-\infty}^{\infty} e^{-i(\varepsilon_a-\hat{H}_0)t_1 - n\lambda|t_1|} dt_1 \hat{H}_{\mathrm{int}} \times \left(\frac{1}{\varepsilon_a-\hat{H}_0}\hat{H}_{\mathrm{int}}\right)^{n-1} |\Phi_a\rangle_{\mathrm{irr}} \\
&= -2\pi\delta(\varepsilon_a-\varepsilon_b)\langle\Phi_b| \times \hat{H}_{\mathrm{int}} \left(\frac{1}{\varepsilon_a-\hat{H}_0}\hat{H}_{\mathrm{int}}\right)^{n-1} |\Phi_a\rangle_{\mathrm{irr}}.
\end{aligned} \tag{A7}$$

Note that in Eq. (A7) we can put $\lambda=0$ from the beginning. Then, comparing Eq. (A7) with Eq. (A6) we arrive at the formulas (12) and (13) given in the text.

APPENDIX B

Here we give some details of our numerical procedure and the accuracy estimates. The main problem in the numerical evaluation of the two- and three-photon exchange graphs

is the summation over the complete Dirac spectrum for the intermediate states. For this purpose we employed the B-spline approach [68], in particular the version developed in [69]. As in [69], we use the following grid to construct B-splines. The ion is inserted into a box with the radius $R=55/Z$ a.u., where Z is the charge of the nucleus. The interval R is divided into J parts $\{t_j\}$ given by

$$t_j = R \exp\left[13\left(\frac{j-1}{J-1}-1\right)\right], \quad j=1,\ldots,J. \tag{B1}$$

Then, adding to these grid points 10 points ($t_j=0, j=-9,\ldots,0$) [68], we get the grid on which we construct the set of B-splines of order 10. The program generating the Dirac spectrum was tested by changing the number of grid points (J) when calculating ''step'' graphs with Coulomb and transverse photons and ''box'' and ''cross'' graphs with Coulomb photons. The number of generated energies was varied between 50 and 70 for positive and for negative parts of the spectrum. The variations led to an error less than $\epsilon=10^{-4}$ a.u.

In order to separate the angular variables for the calculation of the matrix element $I^g(\Omega)_{abcd}$, the operator $I^g(\Omega,r_{12})$ [see Eqs. (16), (17), and (23)] is expanded in partial waves. The angular integration is done analytically. The integration over $|\mathbf{r}_1|$ and $|\mathbf{r}_2|$ is done numerically. The interval of integration $[0,R]$ is divided into four parts, which are defined by Eq. (B1) with $J=4$, and on each part the integration is performed using the Gauss rules (with a Legendre polynomial of order $30-40$). In the expansion of the operator I^g only the first 10 partial waves for the two-photon exchange and the first three partial waves for the three-photon exchange were rigorously taken into account. In the case of the two-photon exchange, the remainder of the expansion was evaluated using its asymptotic form. We suppose that the terms of the partial wave expansion drop down as $1/k^3$, where k is the number of the partial wave. For the three-photon case the remainder appeared to be smaller than the accepted error and was omitted.

To perform the integration over Ω in the singular integrals presented in Eqs. (24) and (25), a special procedure was used. Since the integral is convergent for large Ω values, we limit the integration by some finite interval. Then we divide this interval into intervals $\Delta_k=[10k,10(k+1)]$, where k varies between $k_{\max}$ and $k_{\min}$. The values of $k_{\max}$ and $k_{\min}$ in each case are defined by the condition that the contribution of the intervals $\Delta_{k_{\max}}$ and $\Delta_{k_{\min}}$ is smaller than the accepted error of the calculation ($\epsilon=10^{-4}$ a.u.).

The integration over the arbitrary interval Δ_k was performed as follows. Interchanging the order of the summation and integration in Eq. (24), we obtain the integral where the integrand contains many singularities defined by the conditions

$$\Omega=\beta_{n_2}, \beta_{n_2}=\varepsilon_{n_2}-\varepsilon_{b'}. \tag{B2}$$

If $\beta_{n_2}\notin\Delta_k$, the corresponding term of the sum over n_2 is not singular within Δ_k. The numerical integration of such terms will be discussed below. We will designate the singular terms with an asterisk at the sum symbol. Consider the following identity:

$$\int_{\Delta_k}\sum_{n_1 n_2}^{*}\frac{f(\Omega)}{\Omega-\beta_{n_2}+i\,0\varepsilon_{n_2}}d\Omega = \int_{\Delta_k}\sum_{n_1 n_2}^{*}\left\{\frac{f(\Omega)-f(\beta_{n_2})}{\Omega-\beta_{n_2}}+\frac{f(\beta_{n_2})}{\Omega-\beta_{n_2}+i\,0\varepsilon_{n_2}}\right\}d\Omega, \tag{B3}$$

where

$$f(\Omega)=\sum_{gg'}\frac{i}{2\pi}\frac{I^g(\Omega)_{a'b'n_1n_2}I^{g'}(\Omega-\varepsilon_{a'}+\varepsilon_a)_{n_1n_2ab}}{(\varepsilon_a+\varepsilon_b-\varepsilon_{n_1}-\varepsilon_{n_2})}. \tag{B4}$$

The first term in the curly brackets on the right-hand side of Eq. (B3) is nonsingular within Δ_k and can be integrated together with the terms $\beta_{n_2}\notin\Delta_k$. The second term was integrated analytically.

It appeared to be convenient to add points $\{\beta_{n_2}\}$ to the integration grid to make the first term on the right-hand side of Eq. (B3) continuous with the first derivative. We designate the new intervals as δ_l, and l varies between $l_{\max}$ and $l_{\min}$, which are defined by the condition that the intervals $\{\delta_l\}$ compose the same interval of integration as the intervals $\{\Delta_k\}$.

In order to evaluate the integrals in Eqs. (24) and (25) with the desired accuracy $\epsilon=10^{-4}$, we have to calculate the integral on every new interval δ_l with the accuracy

$$\epsilon_l=\epsilon\frac{|F_l|}{\sum_{l'=l_{\min}}^{l_{\max}}|F_{l'}|}, \tag{B5}$$

where F_l is the estimate of the contribution of interval δ_l. This estimate can be given roughly by the integration with two grid points (the end points of δ_l) in which the integrated function in any case has to be calculated. Due to the necessity of monitoring the accuracy for every interval of integration, the Simpson method of integration was used. The number of grid points was increased unless the accuracy ϵ_l was achieved.

[1] R. Marrus, A. Simionovici, P. Indelicato, D. Dietrich, P. Charles, J.P. Briand, K. Bosch, D. Liesen, and F. Parente, Phys. Rev. Lett. **63**, 502 (1989).
[2] B. Birkett, J.P. Briand, P. Charles, D. Dietrich, K. Finlayson, P. Indelicato, D. Liesen, R. Marrus, and A. Simionovichi, Phys. Rev. A **47**, R2454 (1993).
[3] E.G. Myers, J.K. Thomson, E.P. Gavathas, N.R. Claussen, J.D. Silver, and D.J.H. Howie, Phys. Rev. Lett. **75**, 3637 (1995).
[4] R. Marrs, S.E. Elliot, and T. Stöhlker, Phys. Rev. A **52**, 3577 (1995).
[5] T. Stöhlker and A.E. Livingston, Acta Phys. Pol. B **27**, 441 (1996).
[6] J.K. Thomson, D.J.W. Howie, and E.G. Myers, Phys. Rev. A **57**, 180 (1998).
[7] S.D. Bergeson, A. Balakrishnan, K.G.H. Daldwin, T.B. Lucatorto, J.P. Marangos, T.J. McIlrath, T.R. O'Brian, S.L. Rolston, C.J. Sansonetti, J. Wen, N. Westbrook, C.H. Cheng, and E.E. Eyler, Phys. Rev. Lett. **80**, 3475 (1998).
[8] E.G. Myers, H.S. Margolis, J.K. Thompson, M.A. Farmer, J.D. Silver, and M.R. Tarbutt, Phys. Rev. Lett. **82**, 4200 (1999).
[9] J. Schweppe, A. Belkacem, L. Blumenfeld, N. Claytor, B. Feinberg, H. Gould, V.E. Kostroun, L. Levy, S. Misava, J.R. Mowat, and M.H. Prior, Phys. Rev. Lett. **66**, 1434 (1991).
[10] C. Brandau, F. Bosch, G. Dunn, B. Franzke, A. Hoffknecht, C. Kozhuharov, P.H. Mokler, A. Müller, F. Nolden, S. Schippers, Z. Stachura, M. Steck, T. Stöhlker, T. Winkler, and A. Wolf, Hyperfine Interact. **114**, 45 (1998).
[11] P. Beiersdorfer, A.L. Osterfeld, J.H. Scofield, J.R.C. Lopez-Urrutia, and K. Widmann, Phys. Rev. Lett. **80**, 3022 (1998).
[12] V.A. Yerokhin and V.M. Shabaev, Phys. Lett. A **207**, 274 (1995).
[13] V.A. Yerokhin, A.N. Artemyev, and V.M. Shabaev, Phys. Lett. A **234**, 361 (1997).
[14] A.N. Artemyev, V.M. Shabaev, and V.A. Yerokhin, Phys. Rev. A **56**, 3529 (1997).
[15] S.A. Blundell, Phys. Rev. A **46**, 3762 (1992).
[16] I. Lindgren, H. Persson, S. Salomonson, and A. Ynnerman, Phys. Rev. A **47**, R4555 (1993).
[17] H. Persson, I. Lindgren, S. Salomonson, and P. Sunnergren, Phys. Rev. A **48**, 2772 (1993).
[18] V.A. Yerokhin, A.N. Artemyev, T. Beier, V.M. Shabaev, and G. Soff, J. Phys. B **31**, L691 (1998).
[19] A.N. Artemyev, T. Beier, G. Plunien, V.M. Shabaev, G. Soff, and V.A. Yerokhin, Phys. Rev. A **60**, 45 (1999).
[20] V.A. Yerokhin, A.N. Artemyev, T. Beier, G. Plunien, V.M. Shabaev, and G. Soff, Phys. Rev. A **60**, 3522 (1999).
[21] L. Labzowsky, G. Klimchitskaya, and Yu. Dmitriev, *Relativistic Effects in the Spectra of Atomic Systems* (Institute of Physics, Bristol, 1993).
[22] W.R. Johnson, S.A. Blundell, and J. Sapirstein, Phys. Rev. A **37**, 2764 (1988).
[23] Y. Ishikawa and H.M. Quiney, Phys. Rev. A **47**, 1732 (1993).
[24] A. Ynnerman, J. James, H. Persson, and S. Salomonson, Phys. Rev. A **50**, 4671 (1994).
[25] D.R. Plante, W.R. Johnson, and J. Sapirstein, Phys. Rev. A **49**, 3519 (1994).
[26] S. Blundell, P.J. Mohr, W.R. Johnson, and J. Sapirstein, Phys. Rev. A **48**, 2615 (1993).
[27] I. Lindgren, H. Persson, S. Salomonson, and L. Labzowsky, Phys. Rev. A **51**, 1167 (1995).
[28] V.A. Yerokhin, A.N. Artemyev, V.M. Shabaev, M.M. Sysak, O.M. Zherebtsov, and G. Soff, Phys. Rev. Lett. **85**, 4699 (2000).
[29] V. A. Yerokhin, A. N. Artemyev, V. M. Shabaev, M. M. Sysak, O. M. Zherebtsov, and G. Soff, Philos. Mag. (to be published).
[30] P.J. Mohr and J. Sapirstein, Phys. Rev. A **62**, 052501 (2000).
[31] M. Gell-Mann and F. Low, Phys. Rev. **84**, 350 (1951).
[32] J. Sucher, Phys. Rev. **107**, 1448 (1957).
[33] L.N. Labzowsky, Zh. Éksp. Teor. Fiz. **59**, 167 (1970) [Sov. Phys. JETP **32**, 94 (1970)].
[34] L.N. Labzowsky, J. Phys. B **26**, 1039 (1993).
[35] T.E. Timofeeva and L.N. Labzowsky, Izv. Akad. Nauk SSSR, Ser. Fiz. **40**, 2390 (1981).
[36] L. Labzowsky, V. Karasiev, I. Lindgren, H. Persson, and S. Salomonson, Phys. Scr. **T46**, 150 (1993).
[37] M. Braun and V. Shirokov, Izv. Akad. Nauk SSSR Ser. Fiz. **41**, 2585 (1977) [Bull. Acad. Sci. USSR, Phys. Ser. (Engl. Transl.) **41**, 2585 (1977)].
[38] L.N. Labzowsky and M.A. Tokman, J. Phys. B **28**, 3717 (1995).
[39] L.N. Labzowsky and M.A. Tokman, Opt. Spektrosk. **82**, 240 (1997) [Opt. Spectrosc. **82**, 216 (1997)].
[40] L.N. Labzowsky and M.A. Tokman, Adv. Quantum Chem. **30**, 393 (1998).
[41] V.M. Shabaev, Teor. Mat. Fiz. **82**, 83 (1990) [Theor. Math. Phys. **82**, 57 (1990)].
[42] V. Shabaev and I. Fokeeva, Phys. Rev. A **49**, 4489 (1994).
[43] W.H. Furry, Phys. Rev. **81**, 115 (1951).
[44] M. G. Veselov and L. N. Labzowsky, *Teorija Atoma. Strojenie Elektronnykh Obolochek* (*English translation: Theory of Atoms. The Structure of the Electron Shells*) (Nauka, Moscow, 1986) (in Russian).
[45] M. A. Braun, A. D. Gurchumelia, and U. I. Safronova, *Reljativistskaya Teorija Atoma* (*English translation: Relativistic Theory of Atoms*) (Nauka, Moscow, 1984) (in Russian).
[46] V.M. Shabaev, Phys. Rev. A **50**, 4521 (1994).
[47] V. M. Shabaev, Phys. Rep. (to be published), e-print physics/0009018.
[48] A. I. Akhiezer and V. B. Berestetskii, *Quantum Electrodynamics* (Wiley Interscience, New York, 1965).
[49] V. Weisskopf and E. Wigner, Z. Phys. **63**, 54 (1930).
[50] F. Low, Phys. Rev. **88**, 53 (1951).
[51] L.N. Labzowsky, Zh. Éksp. Teor. Fiz. **85**, 869 (1983) [Sov. Phys. JETP **58**, 503 (1983)].
[52] V.G. Gorshkov, L.N. Labzowsky, and A.A. Sultanaev, Zh. Éksp. Teor. Fiz. **96**, 53 (1989) [Sov. Phys. JETP **69**, 28 (1989)].
[53] V.V. Karasiev, L.N. Labzowsky, A.V. Nefiodov, V.G. Gorshkov, and A.A. Sultanaev, Phys. Scr. **46**, 225 (1992).
[54] L. Labzowsky, V. Karasiev, and I. Goidenko, J. Phys. B **27**, L439 (1994).
[55] L.N. Labzowsky, I.A. Goidenko, and D. Liesen, Phys. Scr. **56**, 271 (1997).
[56] L.N. Labzowsky and A.O. Mitrushenkov, Phys. Rev. A **53**, 3029 (1996).
[57] W.R. Johnson and G. Soff, At. Data Nucl. Data Tables **33**, 405 (1985).
[58] P.J. Mohr, Phys. Rev. A **46**, 4421 (1992).

[59] P.J. Mohr and G. Soff, Phys. Rev. Lett. **70**, 158 (1993).
[60] G. Soff and P.J. Mohr, Phys. Rev. A **38**, 5066 (1988).
[61] A.N. Artemyev, V.M. Shabaev, and V.A. Yerokhin, Phys. Rev. A **52**, 1884 (1995).
[62] G.W. Drake, Can. J. Phys. **66**, 586 (1988).
[63] I. Goidenko, L. Labzowsky, A. Nefiodov, G. Plunien, G. Soff, and S. Zschocke, in Proceedings of Hydrogen Atom II: Precision Physics of Simple Atomic Systems, edited by S. G. Karshenboim, R. Pavone, G. Bassani, M. Inguscio, and T.W. Hänsch (Springer, Berlin, in press).
[64] A. Mitrushenkov, L. Labzowsky, I. Lindgren, H. Persson, and S. Salomonson, Phys. Lett. A **200**, 51 (1995).
[65] T. Beier, P.J. Mohr, H. Persson, G. Plunien, M. Greiner, and G. Soff, Phys. Lett. A **236**, 329 (1997).
[66] O.M. Zherebtsov, V.M. Shabaev, and V.A. Yerokhin, Phys. Lett. A **277**, 227 (2000).
[67] V. A. Yerokhin, A. N. Artemyev, V. M. Shabaev, M. M. Sysak, O. M. Zherebtsov, and G. Soff (unpublished).
[68] W.R. Johnson, S.A. Blundell, and J. Sapirstein, Phys. Rev. A **37**, 307 (1988).
[69] L.N. Labzowsky and I.A. Goidenko, J. Phys. B **30**, 177 (1997).
[70] P.J. Mohr, G. Plunien, and G. Soff, Phys. Rep. **293**, 227 (1998).
[71] T. Franosch and G. Soff, Z. Phys. D: At., Mol. Clusters **18**, 219 (1991).
[72] H. Persson, I. Lindgren, S. Salomonson, and P. Sunnergren, Phys. Rev. A **52**, 1884 (1995).
[73] A.V. Neviodov, L.N. Labzowsky, G. Plunien, and G. Soff, Phys. Lett. A **222**, 227 (1996).
[74] S.A. Blundell, Phys. Rev. A **47**, 1790 (1993).
[75] Y.K. Kim, D.H. Baik, P. Indelicato, and J.P. Desclaux, Phys. Rev. A **44**, 148 (1991).
[76] U. Staude, P. Bosselmann, R. Büttner, D. Horn, K.H. Schartner, F. Folkmann, A.E. Livingston, T. Ludziejewski, and P.H. Mokler, Phys. Rev. A **58**, 3516 (1998).